Journal of Cleaner Production 324 (2021) 129143

Contents lists available at ScienceDirect

Journal of Cleaner Production

journal homepage: www.elsevier.com/locate/jclepro

Combined Oscillating Water Column & hydrogen electrolysis for wave energy extraction and management. A case study: The Port of Motril (Spain)

F. Huertas-Fernández [a,*], M. Clavero [a], M.Á Reyes-Merlo [b], A. Moñino [a]

[a] Andalusian Institute for Earth System Research, Universidad de Granada, Av. del Mediterráneo s/n, 18006, Granada, Spain
[b] Técnico Superior de Proyectos y Obras, Demarcación de Costas en Asturias, Dirección General de la Costa y el Mar, Ministerio para la Transición Ecológica y el Reto Demográfico, Spain

ARTICLE INFO

Handling Editor: Cecilia Maria Villas Bôas de Almeida

Keywords:
Wave power
OWC
Green–Hydrogen
Electrolysis
Ports
Net present value

ABSTRACT

This paper presents a theoretical novel approach to a marine infrastructure, which jointly uses an OWC (Oscillating Water Column) and hydrogen electrolysis as a clean source of primary conversion for energy management, capable to satisfy a continuous designed demand. A case study in the Port of Motril (Southern Spain) is proposed in order to analyze the performance of the power plant. The assessment covers the sale and management profits from the harvested energy from waves in the electricity market, and from the electrolysis of the oceanic water H_2O plus dissolved salts μ into hydrogen H_2, oxygen O_2 and salts μ components, also known as green hydrogen.

The investment analysis of the project is conducted through the dynamic financial index Net Present Value (NPV), using Monte Carlo techniques to determine the repayment period. The results are consistent, showing that the plant could supply the annual electricity demand of 356 people with a short repayment period. The amount of energy depends on peak periods T_p and wave heights H_s, which means that other locations could be found so as to improve the performance of the plant in terms of productions of energy and demand supply.

1. Introduction

The current issue of decarbonization and the energy demand of today's society require civil infrastructures, with clean production sources and efficient storage, and scalable in terms of power demand and land management.

One of these sources is wave energy, which transforms the energy of waves into electricity. Due to its significance, this work focuses on both the Oscillating Water Column technology (hereinafter OWC) for wave energy extraction and management, and in its combined use with hydrogen electrolysis technology with a twofold purpose: the sale in the electricity market and the conversion of H_2O water into H_2 and O_2 via electrolysis for further processing. The OWC technology has been extensively studied and introduced as a reliable energy source in recent decades, Cruz (2008). On the other hand, hydrogen H_2 is being considered as a future alternative for power transformation. Through its reaction with oxygen – an exothermic process releasing an energy of 1.4×10^8 J $kg^{-1,a}$ – it provides electric power to be stored and transported/distributed later. Indeed, the availability of ocean water and the feasibility of using electrolysis, Blanco-Fernández and Pérez-Arribas (2017), allow for clean and scalable energy management.

As a brief summary on the OWC context, the analytical solution of the radiation–diffraction problem for the waves impinging the OWC structure and driving its power take-off system, has been developed using Linear Theory, Evans (1982), Sarmento and Falcão (1985) and Evans and Porter (1995). In a step further, the radiation–diffraction problem has been enhanced with specific thermodynamic considerations for the dry air and water vapor mixture driving the OWC system, Medina-Lopez et al. (2019). Research on the boundary conditions of the OWC system have been extensively developed by Martins-Rivas and Mei (2009) and Lovas et al. (2010), among others. The mutual influence between sea states and tides and the OWC performance has been considered in López et al. (2014), whereas the optimization of the OWC system design is included in Zhang et al. (2012), and also the influence of the seabed, bottom slope or the changes on the equipment's efficiency, Rezanejad et al. (2015, 2013) and Medina-López et al. (2017a).

In parallel to theoretical developments, numerical models and experimental investigations have been carried out, assessing the dynamics between forcing agents and the OWC device, Teixeira et al. (2013) and Moñino et al. (2017). The study of efficiency with non-linear models has been object of interest, Luo et al. (2014), alongside with

* Corresponding author.
E-mail address: f_hf@outlook.es (F. Huertas-Fernández).

https://doi.org/10.1016/j.jclepro.2021.129143
Received 12 July 2021; Received in revised form 15 September 2021; Accepted 20 September 2021
Available online 1 October 2021

the focusing on specific air chamber configurations, Bingham et al. (2015). Indeed, all that knowledge has been essential for a correct characterization of the OWC system and its performance.

From the operational point of view, see Fig. 1, the OWC system mainly consists of a hollow structure exposed to wave action, which is partially submerged into the water and with an opening at its base. The transmission of the wave motion compresses (exhalation) and expands (inhalation) the air inside the chamber, driving an air flow that moves a turbine installed in the outlet duct of the OWC, converting the pneumatic power into electricity.

At this point, this research focuses on the management of the wave power generation with a twofold purpose: the sale in the electricity market and the conversion of H_2O water into H_2 and O_2 via electrolysis.

Regarding the hydrogen electrolysis, the transformation of water H_2O by electrolysis into oxygen O_2 and hydrogen H_2 has been extensively studied since the 18th century, van Troostwijk and Deiman (1789), and used industrially with alkaline technology (Engelhardt, 1904) since the 20th century. In 1789, Paets van Troostwyk and Deinman published the first observations on the decomposition of water by electrical charges into 'air inflammable' – hydrogen – and 'air vital' —oxygen, van Troostwijk and Deiman (1789). During the 19th century, obtaining hydrogen by electrolysis was a cost-effective solution. Professor D. Latchinof in Saint Petersburg and d'Arsonval of the french school developed the first electrolytic systems for industrial use, Guillet and Millet (2015).

In 1885–1887, d'Arsonval used a perforated iron cylinder as anode, a cloth as diaphragm, an electrolyte with a concentration of 30% KOH and he used a cylindrical iron vessel, Hale (1919) of 20 cm diameter and 60 cm high as cathode. The maximum applied current was 60 A corresponding to 16 $mAcm^{-2}$. Oxygen was the only element stored releasing hydrogen. The production capacity of the plant was 100 Nm^3 to 150 Nm^3, Engelhardt (1904). Cdt Renard designed an electrolyzer which had 0.002 m concentric cylindrical steel sheets as electrodes. The innermost sheet was used as anode, with 0.17 m in diameter and 3.29 m in height. The outer sheet of 0.30 m in diameter and 3.40 m in height was used as cathode and as electrolyte tank. Internal resistance was 7.5 $m\Omega$ and the voltage and current was 2.7 V at 365 A. It could produce 158 $NLh^{-1,a}$.

Prof. Latchinov developed the first machine, featuring bipolar electrodes separated by iron sheets, Guillet and Millet (2015). A maximum of 44 electrodes 1.4 m high and 21 cm wide could be operated. The machine was placed into a wooden box where the two protruding plates made contact with the anodes. These plates were connected to the grid with a current density of 100 $mAcm^{-2}$, which created a cell with a voltage of 2.5 V. In 1900, Dr Schimidt patented the first industrial electrizer, Schmidt (1899). The design used asbestos cloths as a diaphragm. Two types of electrolyzers with 44 and 26 electrodes operated at 110 V and 65 V respectively with intensities of 15 A to 150 A, producing 163 NLh^{-1} to 2750 NLh^{-1}. More than 400 industries used this technology to produce hydrogen for cutting and welding due to the high temperature of the oxy-hydrogen welding flame, Kreuter and Hofmann (1998).

In 1920–1930, the demand for hydrogen raised due to the increased use of ammonium [$N_2+3H_2 \rightharpoonup 2NH_3$] in agriculture. The main ammonium manufacturing plants were located in Switzerland, Norway and Canada, because of the availability of low-cost electric power obtained from the waterfalls located in the mountain ranges of these countries. The most important ammonium plant, built in 1947 was operated by Norsk Hydro in Glomfjord (Norway). This facility required 380 MW of hydroelectric power to produce 1300 td^{-1} of ammonium, Da Rosa and Ordonez (2021).

In 1950, hydrocarbons began to be used to produce hydrogen on a large scale by gasification at a much lower cost than electrolysis. The economic advantages of electrolysis diminish and the last factory located in Norway closed in 1992, Guillet and Millet (2015).

In 2010, hydrogen used in industry approached 70 Mty^{-1}, most of it obtained from fossil sources. The distribution of the production would be as follows: 48% from natural gas, 30% refining from waste gases, 18% from coal gasification and 4% from electrolysis, IEA Energy Technology Essen-tials (2007). The food and pharmaceutical industry prefer hydrogen obtained from electrolysis thanks to the purity of the resulting gas, approaching to 99.999%, Guillet and Millet (2015).

The main objective in this research is to demonstrate that a marine work can be enhanced with the technology to supply a continuous demand, using hydrogen electrolysis for energy storage and OWC as a renewable source of primary conversion. It is as a case study the Port of Motril (Spain). To this end, the following specific objectives are also proposed:

- Calculation of the energy required for the conversion of water into hydrogen by means of thermodynamic analysis from equations of elements, water H_2O, hydrogen H_2 and oxygen O_2.
- Calculation of the amount of electrical energy obtained from the OWC system produced by successive sea states, in the analyzed time interval.
- Calculation of the amount of hydrogen produced per sea state through water electrolysis. This hydrogen will be stored for later conversion into electricity.
- Cost–benefit analysis of the proposed project, analyzing its economic viability.
- Calculation of the volume of water dissociated and stored to satisfy the designed demand in the proposed time interval.

2. Methodology and theoretical background

The Fig. 2 shows the diagram of the proposed energy production and storage system followed in this work. Energy from the OWC system as well as any other energy that is available on the network at any given moment, can be stored in the form of hydrogen. The energy supplied to the electrolyzers produces an energy jump in the H_2O system, which leads to the dissociation of the water molecule into hydrogen H_2, oxygen O_2 and salts featured with chemical potential μ. Hence, both gases are stored for later transformation into water, obtaining from this reaction electrical power available for sale in the electricity market. Water from this transformation can be used for dilution salts in it and be returned by emissaries to the ocean.

Therefore, it is possible to distinguish three states (H_2O, H_2, O_2) and two jumps ΔZ_i where Z is one of the extensive thermodynamic variables (U — Internal energy, G — Gibbs potential, H — Enthalpy, F — Helmholtz free energy, S — Entropy). The necessary energy to produce the jump is determined throughout the virtual variations of states. Stored hydrogen and oxygen are considered stored energy, which can be introduced into the electrical network at any time.

Once the plant has been designed and the efficiencies calculated, the investment will be analyzed through dynamic project evaluation techniques. To this purpose, the NPV 'net economic present value' proposed by ROM (2009) is computed to assess the project investment, carrying out verification methods (Monte-Carlo simulations) in order to determine the probable recovery period.

According with the previous scheme, this section is structured as follows. First, a review of the current electrolysis technology is presented, followed by the calculation of the thermodynamic potentials of each element and the energy jump corresponding to 1 kg of water. Next, the study of wave energy extraction is carried out using the OWC system. Finally, the management of stored and sold energy is considered, and the investment analysis is presented.

2.1. Electrolytic technology

The two main technologies that currently exist for electrolysis are PEM (proton exchange membrane) technology and alkaline technology, which are explained in detail in the following sections.

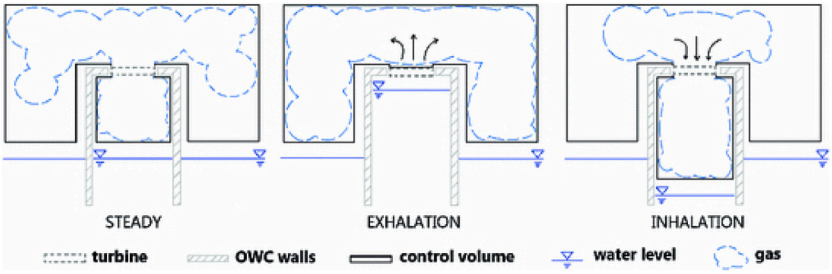

Fig. 1. Operating diagrams of the OWC device, Moñino et al. (2018).

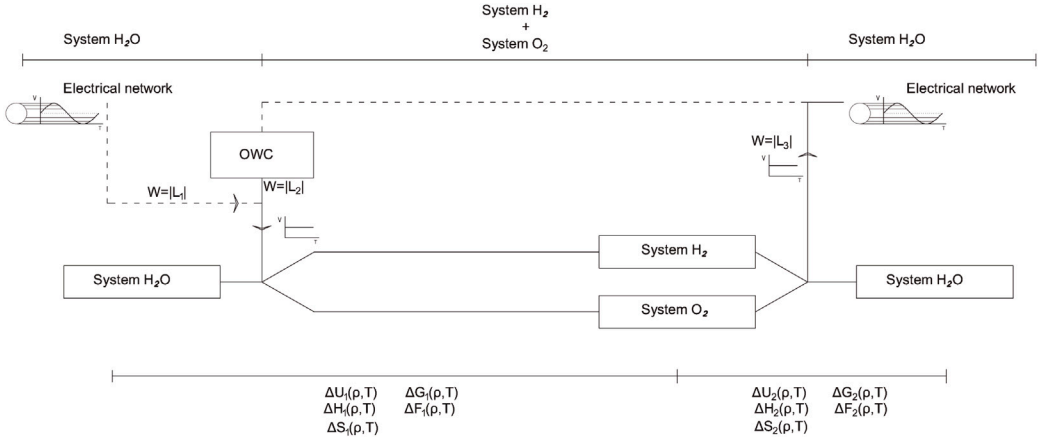

Fig. 2. Methodological scheme.

2.1.1. PEM technology

In the PEM cells, deionized water is used as 'electrolyte'. This restriction of purity limits the operation of these cells in this theoretical model. The core main component of the cell is the proton conducting membrane, with a width of approximately 0.2 mm. These cells are very compact and the electrolysis efficiency is high. The membrane's mission is twofold: as a mean of protons transport and as a physical separator of the two products, preventing their spontaneous exothermic recombination in water. The commonly used material for the membrane is tetrafluoroethylene based fluoropolymer-copolymer, also called Nafion, Grubb (1959).

The membrane is covered with two catalytic layers that are connected to a DC power supply. Electric current is used for the decomposition of water into oxygen at the anode $2H_2O(l) \rightharpoonup O_2(g)+4H^+ +4e^-$. In it solvated protons are produced and these migrate towards the cathode, where they are desolvated and reduced in molecular hydrogen $4H^+ + 4e^- \rightharpoonup 2H_2(g)$. The flow of water through the cell is called electroosmosis, Guillet and Millet (2015).

2.1.2. Alkaline technology

The other main process used to produce the electrolysis is the alkaline technology. This technology has the advantage of using simpler materials over other conversion technologies. Iron or nickel-plated steel is used for hydrogen production (cathode) and nickel for oxygen production (anode). The electrodes are placed in an alkaline aqueous solution and separated by a porous diaphragm that allows the transmission of OH^- between the electrodes. The reaction requires an energy input on the anode with at least a potential difference of $E^{\underline{O}} = 1.23$–2 V, Guillet and Millet (2015). At the anode, the OH^- compounds are oxidized producing oxygen gas $4OH^- \rightharpoonup O_2+2H_2O+4e^-$. At the cathode, a negative polarization is produced and the electrons coming from the electric circuit are used for the water reduction into hydrogen $4H_2O+4e^- \rightharpoonup 2H_2+4OH^-$. In this technology the reaction occurs on the surface of the electrodes. Also, the amount of gas produced is proportional to the electrical flow introduced into the system (Faraday's Law), every four electrons that are provided to two molecules of water, one molecule of oxygen and two of hydrogen are produced. Most of the electrolysers must work with a current density of 10 mol% to 20 mol% power range to guarantee the non-diffusion and mixing of gases inside the electrolyzer (Fick's diffusion law), Guillet and Millet (2015). The hydrogen–oxygen gas explosion occurs in a wide range of concentrations. The lower explosion limit (LEL) is found at a concentration of 3.9 mol% hydrogen in oxygen and its upper explosion limit (UEL) is 95.8 mol%, Schröder and Holtappels (2005) and Holtappels (2002).

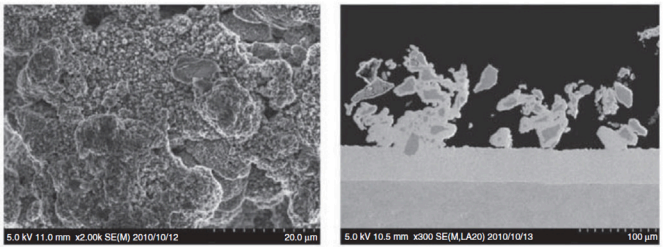

Fig. 3. SEM images of activated Raney nickel catalyst deposited on a Ni mesh substrate, Guillet and Millet (2015).

The volume of electrolyte that is stored in the electromechanical cell is determined by the electrode spacing. These distances are usually between millimeters and centimeters. Ohmic losses increase with the distance between electrodes. Aqueous solutions rich in potassium KOH are preferred over sodium NaOH mixtures because of their higher conductivity. The maximum mixture for conductivity is about 30 wt% which is used for modern electrolyzers, Gilliam et al. (2007) and See and White (1997).

The materials used for the electrodes must resist the corrosion, have a high conductivity and a low cost. It must be a highly catalytic material

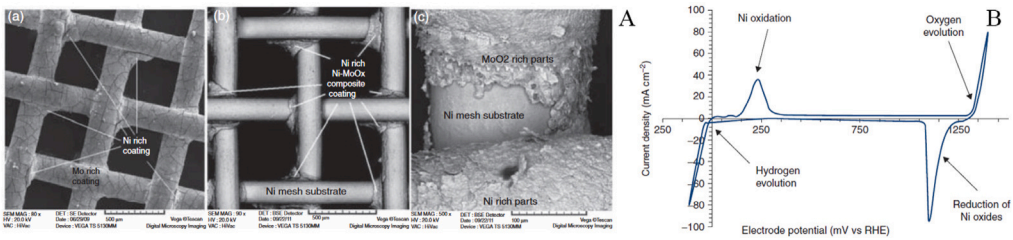

Fig. 4. A: Catalyst (Ni-MoOx and Ni-MoO2) Nickel-Molybdenum oxide and dioxide coated. Ni mesh before (a) after 'service life' test. (b) NiMoOx coating and (c) Ni-MoO2 coating, Guillet and Millet (2015). B: Cyclic voltammetry of a Raney nickel electrode, Guillet and Millet (2015).

to bring the two gases together as quickly as possible in both reactions, 'hydrogen evolution reaction' (HER) and 'oxygen evolution reaction' (OER). Nickel is an electrically stable material, offering high corrosion resistance in alkaline solutions like ocean water at a reasonable cost of 13.8 €kg^{-1}, Mundi. Nickel panels have shown great durability even in conditions of accelerated corrosion where no current is circulating on their surface. Due to these reasons nickel panels are chosen as catalytic material in this study, other catalytic could have better results in the process of electrolysis but volume necessities of the plant could required big structures comparable to thermal or gas plants for electrolysis obligating to use easily available and easily constructed tested material. Raney patented the process for the synthesis of high purity silicon and nickel which was called 'Raney nickel' Fig. 3, Murray (1925). This 'Raney nickel' is a pure nickel sheet with controlled porosity and great surface area, being this process improved in 1927 adding aluminum, Murray (1927). However, the best formulation that produces a better catalyst has not yet been discovered. Numerous works are investigating for the fastest catalysts through formulations and alloys between one or more metals, Gerken et al. (2014).

Gas evolution in the nickel pores produces losses through oxidation and reduction at both electrodes. In addition to these losses, mechanical stresses occur in the sheets. After switching off the electrolyzer, both electrodes are still charged, measuring different potentials equaling approximately 80 min for an electrolyzer with Raney nickel plates as electrodes that cycle with a potential variation of 1 mV s^{-1}, Gerken et al. (2014). The accumulation of cycles of switching on and off Fig. 4B, which is equivalent to the oxidation and marked reduction of the catalytic element, as well as internal mechanical stresses that are experiencing during the use of the electrolyzer, cause loss on the catalytic elements, Fig. 4A, in the form of Ni-MoOx and Ni-MoO2 that coat on the mesh.

The separator diaphragm Fig. 5 must be a porous and stable material that is installed in the gap between the cathode and anode. Its main mission is the separation of both electrodes and the prevention of the recombination of generated H_2 and O_2, so it must be highly conductive of OH^- ions. The first material used was asbestos plates as diaphragm, though it is not very resistant to corrosion and was declared carcinogenic by the European Union in 1999, European Commision (1999). Since 1970, the combination of stable hydrophobic polymers and hydrophilic ceramics achieves a material with high chemical stability, acceptable mechanical behavior and controlled porosity. The most commonly used material as a separator is a polysulfide net with zirconium oxide Fig. 5A, as an inorganic filler material. The trade name of this diaphragm is Zirfon Perl, Schalenbach et al. (2016) and it was marketed by Agfa-Gevart Group, Agfa. This material contains 85 wt% of hydrophilic ZrO_2 with a high specific surface area of 22 m^{2}g^{-1} and 15 wt% of polysulfide, which gives a mechanically resistant material of 0.5 mm of thickness Fig. 5B. There are two configurations, for high temperature (HT) Zirfon Perl HT and low temperature (LT) Zirfon Perl LT.

The smaller the electrode spacing, the lower the losses of the electrolyzer. Fig. 6 shows a schematic of the existing assembly systems. Fig. 6A corresponds to the conventional porous diaphragm model.

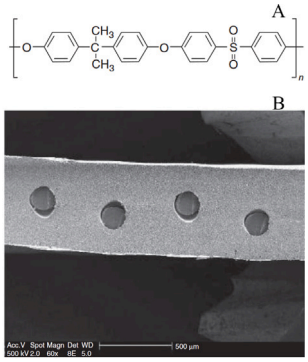

Fig. 5. A: Zirfon Perl LT structure. B: Zirfon Perl LT SEM image cross section of a 500 µm (Guillet and Millet, 2015).

In Fig. 6B the assembled model with no space between electrodes 'zero-gap' is presented, in which the electrodes are placed in direct contact with the porous sheet in order to reduce their losses, the assembly of these cells is more complicated but higher current density and lower losses are achieved, Costa and Grimes (1967), Wendt and Hofmann (1985). Anion membrane technology is used for high pressure electrolyzers, Fig. 6C.

2.2. Equations of state

The equations of state of each of the elements (H_2O, H_2, O_2) have been calculated using the Helmholtz free energy $f(\delta,\tau)$ in its dimensionless molar version $\phi = \phi(\delta,\tau)$ Eq. (1), Jaynes (1957). A theoretical review can be found in Appendix A.

$$\phi(\delta,\tau) = \phi^o(\delta,\tau) + \phi^r(\delta,\tau) = \frac{f(\delta,\tau)}{RT} = f^o(\rho,T)/RT + f^r(\rho,T)/RT \quad (1)$$

The variable $\delta = \rho/\rho_c$ is the reduced density and $\tau = T_c/T$ the reduced temperature, ρ_c and T_c are the density and temperature of the critical point. The critical point is a true equilibrium state of the simple system where $\delta u>0$ and in which SCS is in incipient instability state, Gayé (1997). The variable f^o represents the molar free energy or Helmholtz potential for an ideal gas, and f^r is the residual behavior.

Equation of state that describe each element, with the ideal and residual parts, are adjusted from laboratory data. This work uses the equation of each element proposed by NIST for water, Wagner and Pruß (2002), hydrogen, Leachman et al. (2009) and oxygen, Schmidt and Wagner (1985).

2.3. Change of state

A chemical reaction can be defined as a thermodynamic process of a closed system where the masses of its components change one at expense of others, Gayé (1997). Therefore, the mass in a chemical reaction is conserved Eq. (2) (Lavoisier's Law), but not the total number of moles. If M_i is the molecular mass of the component i, and N_i the

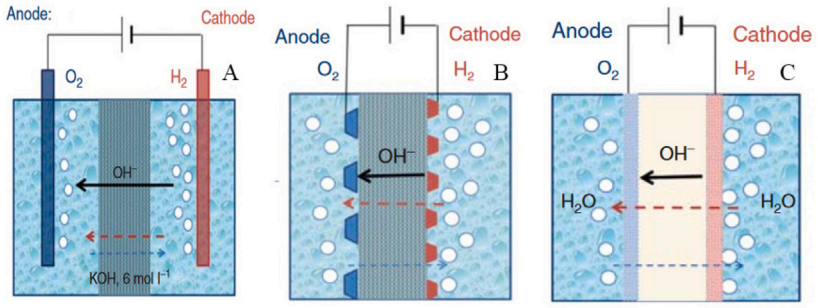

Fig. 6. Typology diagrams of electrolyzers, Guillet and Millet (2015). A: Schematic view of usual electrolysis cell with a porous separator. B: Schematic view of a zero-gap electrolysis cell. C: Schematic view of an alkaline electrolysis cell with anionic diaphragm.

number of moles of the component i, the chemical reaction can be defined as Eq. (3). Considering $\Delta N_i \neq 0$ a chemical reaction can be written as Eq. (4), where ν is the integer number of stoichiometric coefficients of the reaction, ($\nu_i > 0$ if $i > k$ and $\nu_i < 0$ if $i \leq k$) k is the index of change between reactants and products. The variable ζ describes the degree of progress of the reaction with unit *dedonder*. A reaction with $\zeta = 1$ is called the unit reaction. The unit reaction chosen in this paper is 1 kg of water. Therefore, the molar variation of each element of a reaction considering B the products and A the reactants responds to Eq. (5).

$$\sum_{i=1}^{r} m_i(A) = \sum_{i=1}^{r} m_i(B) \tag{2}$$

$$\sum_{i=1}^{r} M_i \Delta N_i = 0 \tag{3}$$

$$\Delta N_i = \nu_i \zeta \tag{4}$$

$$N_i(B) = N_i(A) + \nu_i \zeta \tag{5}$$

An extensive variable Z is defined by its number of moles multiply by a intensive variable z_i of each component Eq. (6). The change of state experiment by the variable during the electrolysis process can be calculate with Eq. (7). A more exhaustive explication of the change of state calculated in this paper can be found in Appendix A.

$$Z = \sum_{i=1}^{r} N_i z_i \tag{6}$$

$$\Delta Z = \int_0^{\zeta} \frac{dZ}{d\zeta} d\zeta \tag{7}$$

2.4. Maritime climate study

The Port of Motril has been taken as a case study. The port is located in southern Spain, and its main breakwater is made up of vertical concrete caissons Fig. 7.

The OWC system is used to obtain the necessary energy for water electrolysis. For this purpose, a maritime climate study has been carried out in the port of Motril and the energy available and produced during a time window has been calculated. The available maritime data corresponds to SIMAR point 2042080, Puertos (2020). This point is chosen due to its proximity to the port. The available record of 59 years starts in 01-04-1958 and finishes in 15-03-2017. The maritime climate analysis is performed with average and extreme regime. The analyzed variables in this work are the significant wave height H_s, the peak wave period T_p and the incidence direction θ. Linear theory is used to assess wave magnitudes in the selected 10 years time window, in this case from 01-01-1980 to 01-01-1990. Obtaining wave characteristics (wave height, wave period and incident direction) in front of the breakwater, E average spatial energy and P power can be calculated by Eqs. (8) and (9).

$$E = \frac{1}{8} \rho g H_2^2 \tag{8}$$

$$P = \frac{1}{8} g \rho C_g \mathrm{H}_2^2 \tag{9}$$

2.5. Implementation of the OWC system

The formulation presented in this work to compute the pneumatic power P_n Eq. (10) is the classic formulation, Martins-Rivas and Mei (2009), in which the air flux through the turbine is determined as a function of a pressure drop in the chamber. The displacement of the water surface Q through the turbine coincides with the flow generated by the water column inside the chamber. A harmonic motion entails $Q = \Re(\hat{Q}e^{-i\omega t})$ and $p = \Re(\hat{p}e^{-i\omega t})$, being $\hat{Q}$ the upward flux water surface in a time step (Martins-Rivas and Mei, 2009) which involves a pressure variation $\hat{p}$ Eq. (11). C_s is the speed of sound in air where $C_s = (\partial p/\partial t)^{1/2}$, k is a turbine parameter, D is the diameter of the turbine, N_v is the number of laps, ρ_a is the density of air and ω the frequency.

The first potential of Eq. (11) is due to the oscillations of the water column inside the chamber and the second to the presence of a structure on which a train of wave impacts. At the same time as the water rises inside the chamber, the radiation $\hat{Q}^R$ and diffraction $\hat{Q}^D$ problem occurs Eq. (12).

$$P_n = \frac{1}{T_p} \int_0^{\frac{2\pi}{\omega}} Q(t)p(t)dt \tag{10}$$

$$\hat{Q} = \left(\frac{kD}{N_v \rho_a} - \frac{i\omega V}{C_s^2 \rho_a} \right) \hat{p} \tag{11}$$

$$\hat{Q} = \hat{Q}^R + \hat{Q}^D \tag{12}$$

2.6. Efficiency

The efficiency η relates the supplied and the obtained energy of the system. In general, the efficiency of a machine is called the quotient between the 'desired' energy and the 'necessary' energy, where 'necessary energy $\|Q_1\|$ = desired energy $\|L\|$ + unavoidable energy $\|Q_2\|$', Gayé (1997). The set of systems that evolve cyclically is called auxiliary system (AS) of a thermodynamic machine, which is called a heat engine if it provides useful work, Gayé (1997). Table 1 shows the formulation and Fig. 8 the calculation scheme of the proposed system.

Fig. 7. Port of Motril: situation and main breakwater. Source: Motril Port Authority.

Table 1
Efficiency table, Gayé (1997).

Machine	$\Delta U^{A,S}$	Efficiency	Limits
Engine	$\|Q_1\| - \|Q_2\| - \|L\| = 0$	$\eta = \frac{\|L\|}{\|Q_1\|} = 1 - \frac{\|Q_2\|}{\|Q_1\|}$	$0 < \eta < 1$

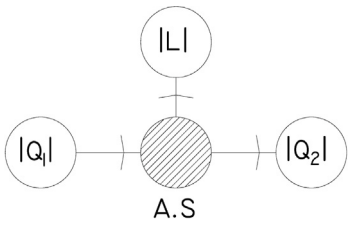

Fig. 8. Operating model scheme, Gayé (1997).

2.7. Investment analysis

According to ROM (2009), the main problems in an investment project are the optimizing of financial profitability in its useful life and the economic effects of the operations and the agents involved. For the calculation, the investment of establishment, maintenance and operation is quantified, bound to the constraints of the technical parameters. The economic net present value NPV_{eco} and NPV_{soc} functions can be optimized, among other economic indexes. These are calculated for each year of the service life obtaining the variations of the economic surpluses of all agents affected by the project using Eqs. (13) and (14).

$NV_{eco,t}$ is the net value in the year t, ∇EO is the surplus of the operators (Port Authority), ∇INV are the investment costs, $\nabla(CO - PM)$ is the difference of opportunity costs and ∇ECL is the customer surplus. The economic net present value and the economic equivalent annual value are obtained with Eqs. (14) and (15), ROM (2009). A statistical risk assessment is conducted by means distribution functions for the evaluation indicator, NPV, applying Monte-Carlo simulations, a level III method used to obtain the solution of the verification equation

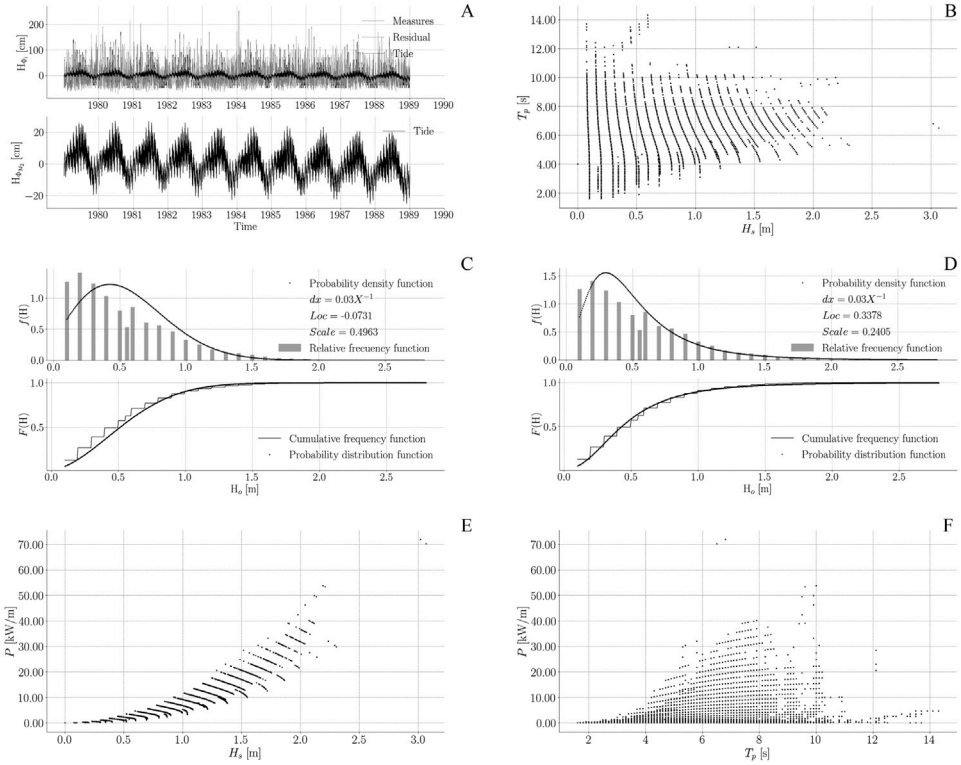

Fig. 9. Maritime climate study. A: Significant harmonics of the localization. B: Dispersion scheme with a average height of $h = 15$ m in front of breakwater. C: Fitted Rayleigh probability function in average regime. D: Fitted Extreme Values probability function in extreme regime. E: Power dispersion with respect to the peak period. F: Power dispersion with respect to the wave height.

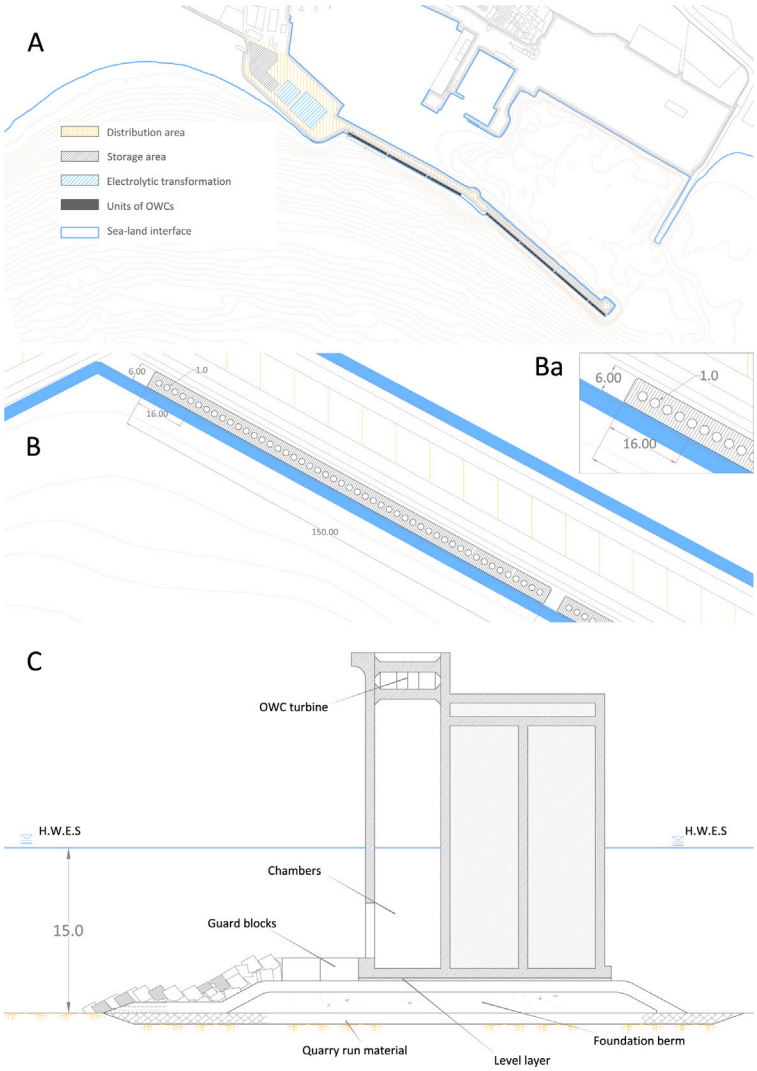

Fig. 10. Model proposed for the port of Motril. A: projected OWC system and distribution areas. B: OWC module. Ba: Detail OWC unit capture. C: Cross section of breakwater and OWC system.

by integrating a multidimensional function in the failure domain ROM (2009). Following Katrin and Stefan (2011) and Vaughan et al. (2000) the investment of the project has great uncertainty and is dependent on the location of the work as well as the type of public entity that promotes it. Both authors propose a symmetric triangular distribution of uncertainty with an expected value and an estimate of the deviation between 5% and 15%. ∇EO is the cash flow of the operators, which is the result of matching $\nabla EO = IC$, being I income and C costs. The cost function is presented in Eq. (16) where D is the damage function. As income I_ϵ the energy stored in form of hydrogen and sell by its market value. ∇ECL is the customer surplus, which is used for the analysis of the social NPV_{soc} considering the zero-emission of CO_2 into the atmosphere by the production process as a positive externality. It is necessary to recall that this research focuses on the clean management of the energy production process.

In addition, a consideration on the sustainability of this project can be further conducted from the standpoint of exergy balance. Indeed, the authors in this research have presented information on thermodynamic state functions involved in the compression/expansion process inside the OWC chamber, Medina-López et al. (2017b), that allow to carry on with a further exergetic balance analysis. Following the focusing of Sciubba (2007), Rosen (1995) and Corrado (2006), the exergy analysis that can be performed to obtain a relationship between exergy and CO_2 consumption through exergy destruction, provides with an estimation of exergy destruction of $d_{ex} = 0.248$ and an exegetic efficiency of $\eta_{ex} = 0.752$. Moreover, a value of the renewability index λ_{ex} can be calculated, de Oliveira Junior (2013). The renewability index takes into account the reduction of quality of the energy – i.e. exergy destruction – related to efficiency of energy conversion processes and to the source of energy, and it is a function of exergy efficiency. In this case, the value of the index is $\lambda_{ex} = 3.04$, therefore it is greater than 1 and the process is an environmentally favorable one, hence reducing the consumption of CO_2. Conversely, other power plants which use fossil fuel has a λ_{ex} in the range between 0.18 and 0.48, less than 1 and not favorable to environment. Therefore the emissions that in fact are not directly produced by this plant in the process of management of energy, can be further used as a positive externality in the investment analysis.

$$NV_{eco,t} = (\nabla EO - \nabla INV)_t + \nabla(CO - PM)_t + \nabla ECL_t \tag{13}$$

$$NPV_{eco,t} = \sum_{t=x}^{X} \frac{NV_{eco,t}}{(1+r)^{t-x}} \tag{14}$$

$$NPV_{soc,t} = \frac{NPV_{eco,t}}{\sum_{t=x}^{X}(1+r)^{t-x}} \tag{15}$$

$$C_T(D_j) = C_{ta}(D_j) + \sum_{i=0}^{n_p} C_D(D_{j,i}) \tag{16}$$

Table 2
Equilibrium thermodynamic states..

Variable		H_2O	H_2	O_2	Units
Number of Moles	N	55.0	55.0	27.5	mole
Molar mass	M	18.01528	2.01588	31.9988	g mol^{-1}
Mass	m	1.0	0.11111	0.8889	kg
Pressure	p	3961482.471	100469.641	100424.366	N m^2
Entropy	S	0.294	6.259	5.678	kJ K^{-1}
Volume	V	0.001	1.346	0.673	m^3
Internal energy	U	83.0	295.829	168.7	kJ
Enthalpy	H	87.008	430.82	236.268	kJ
Gibbs potential	G	1.007	−1403.213	−1427.269	kJ
Helmholtz Potential	F	−2.954	−1538.203	−1494.836	kJ
Chemical potential	μ	0.0183	−25.513	−51.901	kJ
Isochoric molar heat	cv	4.144	1.135	0.584	kJ K^{-1}
Isobaric molar heat	cp	4.172	1.595	0.816	kJ K^{-1}
Formation Energy	pV	3.961	134.99	67.568	kJ
Caloric energy	TS	86.001	1834.033	1663.537	kJ

2.8. Satisfaction of the demand

The demand satisfaction study is based on the energy that can be supplied to the network and that can be maintained over time. The energy conversion in the OWC is conditioned by the sea state at any moment. Stored energy E_{st} in kWh (increase or decrease) is calculated at differential Δt following Eq. (17). Therefore, the amount of energy stored at each instant is calculated with Eq. (18).

$$\Delta E_{st} = E_{st,t} - E_{st,t-1} = E_{in} - E_{out} \tag{17}$$

$$E_{st,t} = E_{in} - E_{out} + E_{st,t-1} \tag{18}$$

Two assumptions can be made in the demand's analysis, the demand E_{out} is lower than the energy converted by the OWC system, $E_{out} < E_{in}$; or the demand is higher than the energy converted by the OWC, $E_{out} > E_{in}$. In the first case, the surplus energy is fed back into the system and stored in the form of hydrogen ϵ_{st}. In the second situation, the deficit energy is obtained from the previously stored $E_{st,t-1} = \sum_{i=0}^{n} \epsilon_{st,i}$. To optimize and scale the plant to a designed demand, the variable to maximize must be the output energy E_{out} according to expression (19), where the following dependencies are proposed: the E_{in} depends on F the energy input that could come from any renewable source in this case the OWC system which depend on wave heights H_s, peak period T_o and technical OWC parameters. On the other hand, the variable ΔE_{st} depends on the storage area S_p, the design demand D, the stored energy ϵ_{st} and efficiency of hydrogen conversion E_{el}.

$$max\{E_{out}\} \quad with \quad E_{out} = E_{in}(F) - \Delta E_{st}(S_p, D, \epsilon_{st}, E_{el}) \tag{19}$$

3. Results

The results of this research are shown in the same order of presentation as in the methodology section, to ease the reading and interpretation.

3.1. Equations of state

The equations of state are presented in Wagner and Pruß (2002) for water, Leachman et al. (2009) for hydrogen and in Schmidt and Wagner (1985) for oxygen, the reduced variables are replaced by their numerical values ($\tau = T_c/T$; $\delta = \rho/\rho_c$). Hence, the equilibrium thermodynamic state defined by density and temperature is shown Table 2 with the extensive values that 1 kg of water H_2O has and its components (0.111 kg of H_2 and 0.889 kg of O_2).

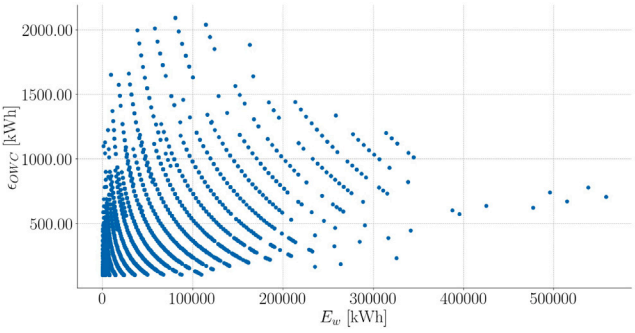

Fig. 11. Relation between incident wave energy and electrical energy obtained by the OWC system.

3.2. Change of state

Eq. (4) is described for each studied element and solving Eq. (7) with Z=G (potential gibbs) which is equal to electrochemical potential or energy required to disassociate 1 kg of water Eq. (20).

$$\Delta G = \int_0^{1\ kgH_2O} \frac{dG}{d\zeta} d\zeta = \|2831.488\|\ kJ \tag{20}$$

3.3. Maritime climate study

The harmonic analysis of the signal Fig. 9A shows that the astronomical tide is less significant from an energetic point of view than the meteorological tide. Hence, wave data is fitted with a Rayleigh probability density function Fig. 9C for the average regime and a density function of Extreme Values Fig. 9D for extreme regime. The dispersion scheme considering $h = 15$ m as the mean of the breakwater bathymetry is shown in Fig. 9B. Power dispersion compared to the peak period is shown Fig. 9F and compared with wave height Fig. 9E. Average wave power of 20 kWm^{-1} can be observed for average return periods of 7 s. It is worth noting the 50 kWm^{-1} recorded for wave heights greater than 2 m. For wave heights corresponding to the astronomical tide is obtained an average power of 0.57 kWm^{-1}.

3.4. Implementation of the OWC system.

Fig. 10A proposes a possible configuration for the implementation of the OWC modules and the areas destined for storage and the electrolysis process in the port of Motril (Spain). This work focuses on geometric limitations and does not consider dynamic or structural implications. The projected modules of the OWC system in this work can be seen in Figs. 10B and 10C. OWC configuration and modules parameters which are been adapted to the configuration and geometry of the port are shown in Table 3.

A set of 10 turbines per module with a power of 30 kW each are planned. Therefore, a power of 300 kW per module can be achieved obtaining a total installed power of 2100 kW = 2.1 MW. Fig. 11 shows the relation between incident wave energy and electrical energy that is obtained by the OWC system ϵ_{OWC}.

3.5. Electrolytic conversion

A 10% of the installed power (210kW) is derived for hydrogen conversion. Therefore, following the relationships presented in Table 3, the potential amount of hydrogen mass created m_{st} is shown in Fig. 12AB. The stored electricity of each kg of hydrogen is calculated according to Eq. (6). Using the data for each species is obtained the stored electrical energy ϵ_{st} Fig. 12CD according to wave height and period respectively. Fig. 13 shows the potential electrical energy that is stored as hydrogen, as can be seen the performance of this conversion is linear due to the lineal shape of electrolysis efficiency.

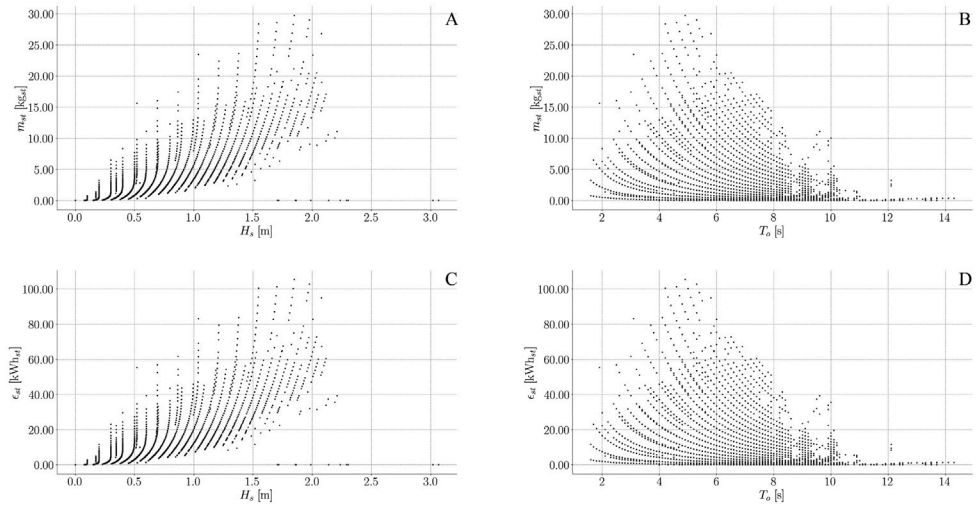

Fig. 12. Potential mass and stored energy as hydrogen: A: Stored potential mass of hydrogen as function of height wave. B: Stored potential mass of hydrogen as function of period wave. C: Stored potential electric energy as function of height wave. D: Stored potential electric energy as function of period wave.

Table 3
OWC configuration parameters.

Description	Variable	Value	Units
Submerged distance	d	10	m
OWC chamber surface	S_{owc}	96	m^2
Submerged water volume	V_o	1430	m^3
Turbine parameter Martins-Rivas and Mei (2009)	k	0.55	[–]
Turbine diameter	D	1	m
Number of laps	N_l	$1100\frac{2\pi}{60}$	rad s^{-1}
Air density	ρ_a	1.25	kg m^{-3}
Speed of sound in air	C_s	343.2	m s^{-1}
Unit capture length	L_n	16	m
Number of OWC per unit	n_u	10	u
Turbine power	P_{tw}	30	kW
Module capture length	L_{ct}	150	m
Number of modules	n_c	7	u
Total implantation length	L_{Tc}	1050	m

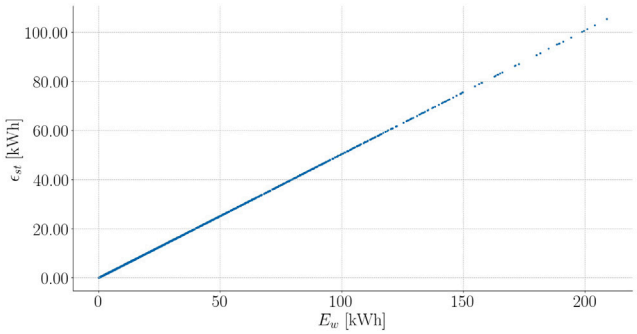

Fig. 13. Electrical energy stored as hydrogen.

3.6. Efficiency

There are two energy conversions in this study. First, the primary energy conversion from the OWC system into electrical energy, and second the energy conversion from electrical energy into hydrogen.

The first conversion, from the incident wave energy train into electrical energy through the OWC system has a efficiency η_{OWC}, that can be interpreted as a function of the wave height and wave period, as shown in Figs. 14A and 14B.

As noted in Guillet and Millet (2015), alkaline technology has a conversion efficiency that ranges from 50% to 67%. The obtained efficiency values η_{el} using the thermodynamic states are displayed with the wave height in Fig. 14C and the wave period in Fig. 14D. As can be seen, this magnitude is not dependent neither on H_s nor on T_o, as it is an electrical conversion.

Table 4
Satisfaction of the demand.

E_{out}	$E_{st,t-1}$	C. Annual per capita	N.pc
1539570.0 kWh y^{-1}	385802.70 kWh$_{st}$	5355.98 kWh pc^{-1} y^{-1}	359 pc

3.7. Investment analysis

The economic net value $NV_{eco,t}$ is calculated with Eq. (13) for the financial $NPV_{eco,t}$ Eq. (14), and the $NPV_{soc,t}$ for the social with Eq. (15). Monte-Carlo techniques are used to estimate the probable number of years in which the investment will be profitable, i.e when the $NPV_{eco,t} = 0$ or $NPV_{soc,t} = 0$. Hence, 100 simulations of 100 years each are run. Random sea states are simulated, for financial Fig. 15A and social Fig. 15B analyses. Once both are calculated, the cumulative frequency and distribution function of the payback period of each index is calculated. Fig. 15C shows the financial $NPV_{eco,t}$ and Fig. 15D shows the social $NPV_{soc,t}$. It should be noted that with a probability of 50% recovers the initial investment in 64 years for financial $NPV_{eco,t}$ while the social $NPV_{soc,t}$ takes 25 years. Partial results as well distribution functions for probabilistic analysis can be seen in Appendix B.

3.8. Satisfaction of the demand

The Fig. 16A shows the energy converted by the OWC system E_{in} and its average in days $\bar{E}_{in}$. Fig. 16B shows the energy stored by electrolysis ϵ_{st} and its average in days $\bar{\epsilon}_{st}$. Fig. 16C shows the variable ΔE_{st} which define the variation of stored energy in the plant and $\dot{V}^{\zeta}_{H_2O}$ volume of dissociated stored water. Fig. 16D shows the system's energy balance in the analyzed windows time. The annual generation of the proposed system is shown in Table 4. Following The World Bank Group, per capita electricity demand for Spain in 2015 is 5355.98 kWh. Therefore, as can be seen, with a base demand E_{out} of 175.75 kWh, supply is guaranteed throughout the analyzed time window, providing energy for a total of 359 people annually.

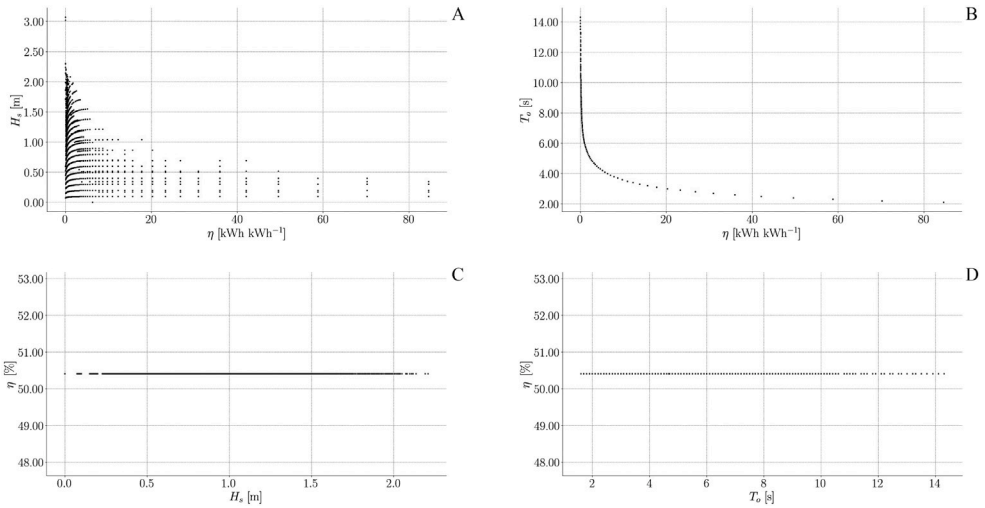

Fig. 14. Conversions efficiencies η_i. A: Efficiency OWC system into electrical energy η_{OWC} as function of wave height. B: Efficiency OWC system into electrical energy η_{OWC} as function of wave period. C: Efficiency of conversion of electrical energy η_{el} into hydrogen as function of wave height. D: Efficiency of conversion of electrical energy η_{el} into hydrogen as function of wave period.

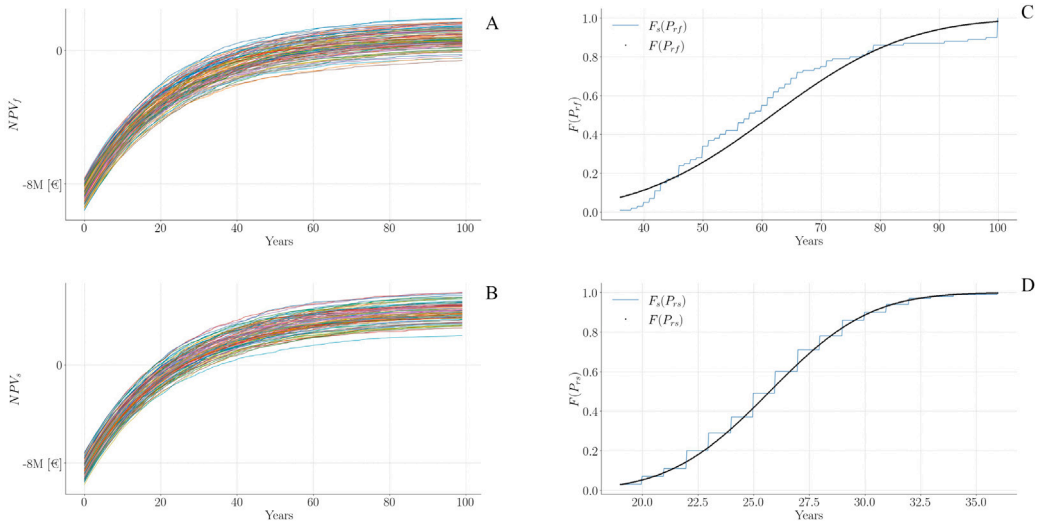

Fig. 15. Investment Analysis. A: $NPV_{soc,t}$ financial analysis. B: $NPV_{eco,t}$ social analysis. C: Distribution function for payback period in financial analysis. Probability distribution function $F(P_{rf})$. Cumulative frequency function $F_s(P_{rf})$. D: Distribution function for payback period in social analysis. Probability distribution function $F(P_{rf})$. Cumulative frequency function $F_s(P_{rf})$.

4. Conclusions

The Table 5 summarizes the computations performed in the previous section, settling the benefits and potential of combining OWC with electrolysis, in order to reach an efficient and cutting edge system inside maritime renewable energy field itself. Indeed, for a given designed demand, the supply is guaranteed. The project has a payback period of approximately 25 years of its operation considering social variables and a probability of 50%. Under the proposed circumstances the annually supplied energy is capable of satisfying the demand of a total of 359 people.

The main conclusions drawn from this work are:

- The wave energy can be harvested through OWC technology, achieving efficiencies that, in certain cases, i.e. $T_o <$ 2s, can reach 75%.
- The conversion of electric power from the OWC into H_2 has an efficiency of 50.5% and can be used for energy storage.
- The OWC conversion technology together with electrolysis allows to maintain a designed electrical demand with guaranteed supply.
- The salts from electrolysis can be diluted with the water from joining stored gases and this dilution be diffused in the ocean by emissaries.
- The initial investment for the installation of the OWC technology and the electrolytic elements is recovered through market profits,

Table 5
Main results.

Variable	Value	
ΔG	0,7865 kWh	Energy required to transform 1 kg of water.
η_{OWC}	[0.20 ~ 0.80]	With wave heights [0.2 ~ 2 m].
η_{el}	50.05%	Electrolysis efficiency.
P_{inst}	2100 kW	Installed power.
INV	8.452 M€	Total investment.
$\bar{b}$	13.15 €s.s.$^{-1}$	Average profit by sea state.
$NPV_{eco,t}$	64	Years to be profitable with a 50% probability.
$NPV_{soc,t}$	25	Years to be profitable with a 50% probability.
E_{out}	1.539 GWh	Energy supplied by the plant in one year.

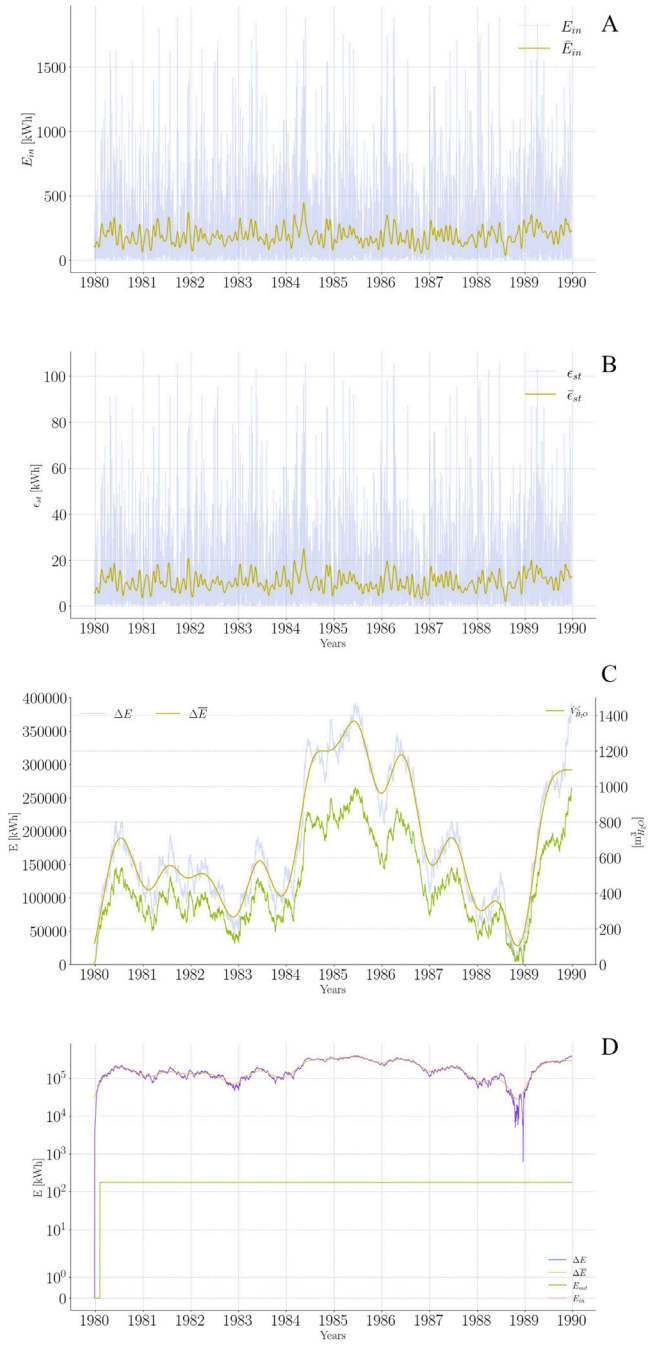

Fig. 16. Satisfaction of demand. A: Energy converted by the OWC system. B: Energy stored by electrolysis. C: Variation of energy stored in the plant and volume of dissociated water. D: Energy balance of the system.

in a relatively short period of time for an infrastructure of its type. In addition, the social impact of the project is considered positive.

- Exergetic balance presents an exergy efficiency of $\eta_{ex} = 0.752$ and an exergy destruction of $d_{ex} = 0.248$ with a renewability index of $\lambda_{ex} = 3.04$.

The methodology presented in this work can be easily applied to any maritime area. Improved results are feasible to be achieved in areas where the maritime climate, energetic potential and wave conditions be different.

The availability of ocean water and clean production sources, alongside with marine, hydraulic and electrical infrastructures respectful with the environment, can provide with clean power facilities to supply demands of energy, even large ones, helping to answer the requirements and necessities of clean energy management from today's and future society.

Table 6
Thermodynamic potentials.

Changes	Definition	Name
$S \to T$	$F \equiv U - TS$	Free energy or Helmholtz potential
$V \to -P$	$H \equiv U + PV$	Enthalpy
$S \to T\ ; V \to -P$	$G \equiv U - TS + PV$	Gibbs potential or free enthalpy

CRediT authorship contribution statement

F. Huertas-Fernández: Concept and idea, Formal analysis, Research, Methodology and coastal and environmental focusing, Writing – original draft – review & editing. **M. Clavero:** Methodology and coastal and environmental focusing, Writing – review & editing. **M.Á Reyes-Merlo:** Methodology and coastal and environmental focusing, Writing – review & editing. **A. Moñino:** Project leading, Formal analysis, Research, Methodology and coastal and environmental focusing, Writing – review & editing.

Declaration of competing interest

The authors declare that they have no known competing financial interests or personal relationships that could have appeared to influence the work reported in this paper.

Appendix A. Methodology and theoretical background

A.1. Equation of state

Each state is defined by thermodynamic state functions in accordance with the following Thermodynamic Postulates, (Gayé, 1997):

- *I.* There are equilibrium states of a simple one-component system (SCS) and they are fully characterized by the following extensive state values $\{U, V, N\}$, energy, volume and number of moles, respectively.
- *II.* There is a state function of an SCS called entropy S, which is extensive, continuous, differentiable in (U, V, N) and monotonically increasing from U.
- *III.* The entropy of an isolated composite system has the following property: in the absence of any internal bond, the values of the extensive state parameters of the subsystems are those that make the energy of the composite system maximum with the conditions proposed by the remaining bonds.
- *IV.* The entropy of a SCS is zero at absolute zero, a state that satisfies $\left(\frac{\partial S}{\partial U}\right)_{V,N} = \infty$.

The fundamental equation $U = U(S, V, N)$ of an SCS is defined in different ways depending on the used thermodynamic potential. Using the Legendre Transformation (Gayé, 1997), the thermodynamic potentials are the result of replacing the extensive variables in each case by their conjugate variables $(S \to T; V \to -P; N \to \mu)$ where T is the temperature, V is the volume, P is the pressure, N the number of moles and μ the chemical potential, Table 6. Molar magnitudes are the quotient of the extensive variables by the number of moles, Table 7.

Thermodynamic properties can be obtained from the fundamental function f Table 9 and its fundamental derivations Table 8 . The computed thermodynamic variables using (NIST; Leachman et al., 2009; Wagner and Pruß, 2002; Schmidt and Wagner, 1985) see Tables 10–12.

Table 7
Molar magnitudes.

Magnitude	Equation
Molar energy	$u \equiv U/N$
Molar entropy	$s \equiv S/N$
Molar volume	$v \equiv V/N$
Molar Helmholtz potential	$f \equiv F/N$
Molar enthalpy	$h \equiv H/N$
Molar Gibbs potential	$\mu \equiv G/N$

Table 8
Fundamental derivations, Wagner and Pruß (2002).

Magnitude	i	j
ϕ^i_j	$i : \{^o\ ideal\ ;\ ^r\ residual\}$	$j : \delta \rightarrow \phi^i_\delta = (\partial\phi^i/\partial\delta)_\tau$ $j : \delta\delta \rightarrow \phi^i_{\delta\delta} = (\partial^2\phi^i/\partial\delta^2)_\tau$ $j : \tau \rightarrow \phi^i_\tau = (\partial\phi^i/\partial\tau)_\delta$ $j : \tau\tau \rightarrow \phi^i_{\tau\tau} = (\partial^2\phi^i/\partial\tau^2)_\delta$

Table 9
Thermodynamic properties and other fundamental functions.

Magnitude	Equation
Pressure Mpa	$p = \rho^2(\partial f/\partial\rho)_T$
	$p(\delta,\tau)/\rho RT = 1 + \delta\phi^r_\delta$
Molar entropy kJ kg^{-1} K^{-1}	$s = -(\partial f/\partial T)_\rho$
	$s(\delta,\tau)/R = \tau(\phi^o_\tau + \phi^r_\tau) - \phi^o - \phi^r$
Molar internal energy kJ kg^{-1}	$u = f + Ts$
	$u(\delta,\tau)/RT = \tau(\phi^o_\tau + \phi^r_\tau)$
Molar enthalpy kJ kg^{-1}	$h = u + pv$
	$h(\delta,\tau)/RT = \tau(\phi^o_\tau + \phi^r_\tau) + \delta\phi^r_\delta$
Molar Gibbs free energy kJ kg^{-1}	$g = h - Ts$
	$g(\delta,\tau)/RT = 1 + \phi^o + \phi^r + \delta\phi^r_\delta$
Isobaric molar heat kJ kg^{-1} K^{-1}	$c_p = (\partial h/\partial T)_p$
	$c_p(\delta,\tau)/R = -\tau^2(\phi^o_{\tau\tau} + \phi^r_{\tau\tau}) + \frac{(1+\delta^r_\delta - \delta\tau\phi^r_{\delta\tau})^2}{1+2\delta\phi^r_\delta + \delta^2\phi^r_{\delta\delta}}$
Isocoric molar heat kJ kg^{-1} K^{-1}	$c_v = (\partial u/\partial T)_\rho$
	$c_v(\delta,\tau)/R = -\tau^2(\phi^o_{\tau\tau} + \phi^r_{\tau\tau})$

Table 10
Fit to the equation of state for H_2O, NIST, Wagner and Pruß (2002).

H_2O
$\phi^o = ln(\delta) + n^o_1 + n^o_2\tau + n^o_3 ln(\tau) + \sum_{i=4}^{8} n^o_i ln[1 - \exp(-\gamma^{o\tau}_i)]$
$\phi^r = \sum_{i=1}^{7} n_i\delta^{d_i}\tau^{t_i} + \sum_{i=8}^{51} n_i\delta^{d_i}\tau^{t_i}\exp(-\delta^{c_i}) +$
$\sum_{i=52}^{54} n_i\delta^{d_i}\tau^{t_i}\exp(-\alpha_i(\delta-\epsilon_i)^2 - \beta_i(\tau-\gamma_i)^2) + \sum_{i=55}^{56} n_i\Delta^{b_i}\delta\psi$
$\Delta = \theta^2 + B_i[(\delta-1)^2]^{a_i}$
$\theta = (1-\tau) + A_i[(\delta-1)^2]^{1/(2\beta_i)}$
$\psi = \exp -C_i(\delta-1)^2 - D_i(\tau-1)^2$

Table 11
Fit to the equation of state for H_2, NIST, Leachman et al. (2009).

H_2
$\phi^o = ln(\delta) + 1.5ln(\tau) + a_1 + a_2\tau + \sum_{k=3}^{N} a_k ln[1 - \exp(b_k\tau)]$
$\phi^r = \sum_{i=1}^{l} N_i\delta^{d_i}\tau^{t_i} + \sum_{i=l+1}^{m} N_i\delta^{d_i}\tau^{t_i}\exp(-\delta^{p_i}) +$
$\sum_{i=m+1}^{n} N_i\delta^{d_i}\tau^{t_i}\exp(-\varphi_i(\delta - D_i)^2 - \beta_i(\tau-\gamma_i)^2)$

Table 12
Fit to the equation of state for O_2, NIST, Schmidt and Wagner (1985).

O_2
$\phi^o = k_1\tau^{1.5} + k_2\tau^{-2} + k_3 ln(\tau) + k_4\tau + k_5 ln(\exp(k_7\tau) - 1) +$
$k_6 ln(1 + (2/3)\exp(-k_8\tau)) + k_9$
$\phi^r = \sum_{i=1}^{13} n_i\delta^{r_i}\tau^{s_i} + \exp(-\delta_2)\sum_{i=14}^{24} n_i\delta^{r_i}\tau^{s_i} +$
$\exp(-\delta^4)\sum_{25}^{32} n_i\delta^{r_i}\tau^{s_i}$

A.2. Change of state

A chemical reaction can be defined as a thermodynamic process of a closed system where the masses of its components change one at expense of others, Gayé (1997). Therefore, the mass in a chemical reaction is conserved equation (21) (Lavoisier's Law), but not the total number of moles. If M_i is the molecular mass of the component i, and N_i the number of moles of the component i, the chemical reaction can be defined as Eq. (22). Considering Eq. (23) a chemical reaction can be written as Eq. (24), where ν is the integer number of stoichiometric coefficients of the reaction, ($\nu_i > 0$ if $i > k$ and $\nu_i < 0$ if $i \leq k$) k is the index of change between reactants and products. The variable ζ describes the degree of progress of the reaction with unit *dedonder*. A reaction with $\zeta = 1$ is called the unit reaction. If $\zeta > 0$, the unit reaction advances $|\zeta|$ times and if $\zeta < 0$ reaction backs up $|\zeta|$ times. Therefore, the molar variation of a reaction process is shown in Eq. (25). Considering B the products and A the reactants, the progress of the reaction responds to Eq. (26).

$$\sum_{i=1}^{r} m_i(A) = \sum_{i=1}^{r} m_i(B) \tag{21}$$

$$\sum_{i=1}^{r} M_i \Delta N_i = 0 \tag{22}$$

$$\sum_{i=1}^{r} \Delta N_i \neq 0 \tag{23}$$

$$\frac{\Delta N_1}{\nu_1} = \cdots = \frac{\Delta N_k}{\nu_k} = \ldots = \frac{\Delta N_{k+1}}{\nu_{k+1}} = \cdots = \frac{\Delta N_r}{\nu_r} = \zeta \tag{24}$$

$$\Delta N_i = \nu_i\zeta \tag{25}$$

$$N_i(B) = N_i(A) + \nu_i\zeta \tag{26}$$

The composition of a simple multi-component system is expressed by specifying mole fractions of each component x_i Eq. (27), that is, the ratios of its number of moles N_i with the number of total $\sum N_k$. Therefore, given an extensive variable Z, the mean molar property is called the intensive variable z fulfilling Eq. (28). Partial molar property of component i is shown in Eq. (29), being the extensive variable defined in Eq. (6).

$$x_i \equiv \frac{N_i}{\sum_{k=1}^{r} N_k} \rightarrow \sum_{i=1}^{r} x_i = 1 \tag{27}$$

$$z \equiv \frac{Z}{\sum_{k=1}^{r} N_k} \tag{28}$$

$$z_i = \left(\frac{\partial Z}{\partial N_i}\right)_{T,P,N'} \tag{29}$$

To find the extensive variable of the Gibbs potential G of a specie, we take the intensive variable z_i as the chemical potential of the

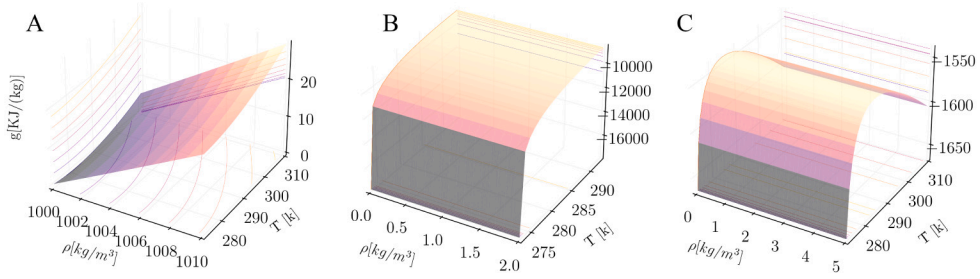

Fig. 17. A: Gibbs potential g of H_2O. B: Gibbs potential g of H_2. C: Gibbs potential g of O_2.

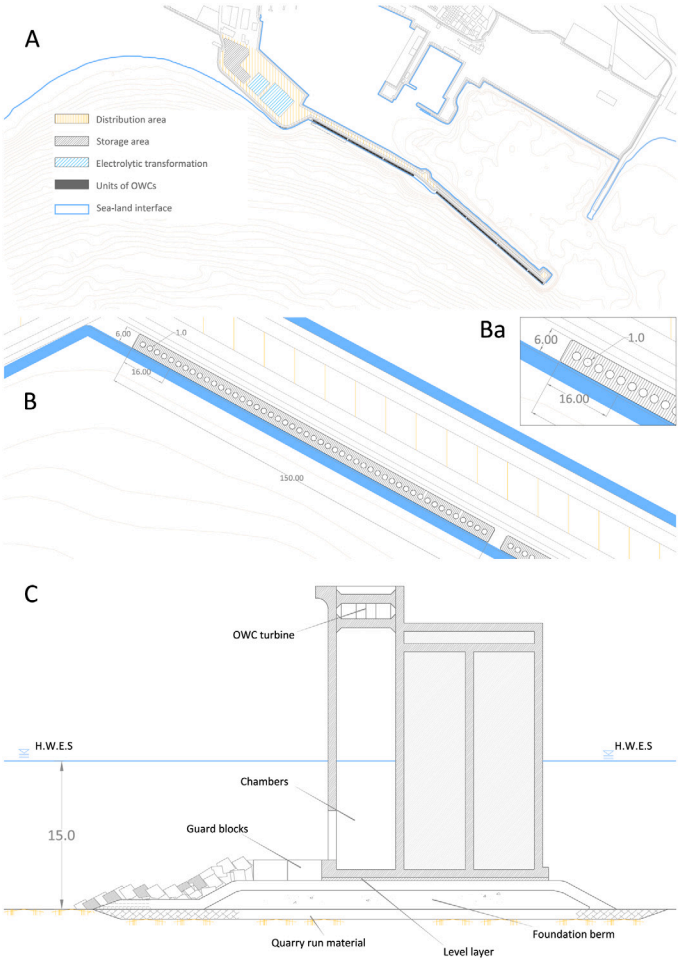

Fig. 18. Model proposed for the port of Motril. A: projected OWC system and distribution areas. B: OWC module. Ba: Detail OWC unit capture. C: Cross section of breakwater and OWC system.

Table 13
Temperature and density of the critical point and ranges of the thermodynamic cells studied.

Element	T_c [K]	ρ_c [mol dm^{-3}]
H_2O	647.096	17.712
H_2	33.145	15.508
O_2	154.599	13.34
Element	**T [K]**	**ρ [kg m^{-3}]**
H_2O	273 – 310	1000 – 1010
H_2	273 – 310	0.0001 – 2
O_2	273 – 310	0.0001 – 5

specie μ which is multiplied by the number of moles of the specie. The chemical potential is related to the electrical power through the equation $\mu_B^\alpha = \hat{\mu_i}^\alpha - z_B F \phi^\alpha$, Gayé (1997). For reactions in which there is no change of species $z_B = 0$ the electrochemical potential is equal to the chemical potential, Renner (2007). Let $Z = Z(T, P, N_i)$ and $Z = Z(S, V, N_i)$ where Z is an extensive variable represented in (T, P, N_i) and (S, V, N_i). Applying Euler's theorem in both definitions of Z, Eqs. (30) and (31) can be found.

$$Z(T,P,N_i) = T\left(\frac{\partial Z}{\partial T}\right)_{P,N_i} + P\left(\frac{\partial Z}{\partial P}\right)_{T,N_i} + N_i\left(\frac{\partial Z}{\partial N_i}\right)_{T,P,N'} \tag{30}$$

$$Z(S,V,N_i) = S\left(\frac{\partial Z}{\partial S}\right)_{V,N_i} + V\left(\frac{\partial Z}{\partial V}\right)_{S,N_i} + N_i\left(\frac{\partial Z}{\partial N_i}\right)_{S,V,N'} \tag{31}$$

Using the relationships between the first derivatives of the thermodynamic potentials, Eq. (32) according to Gayé (1997), and substituting

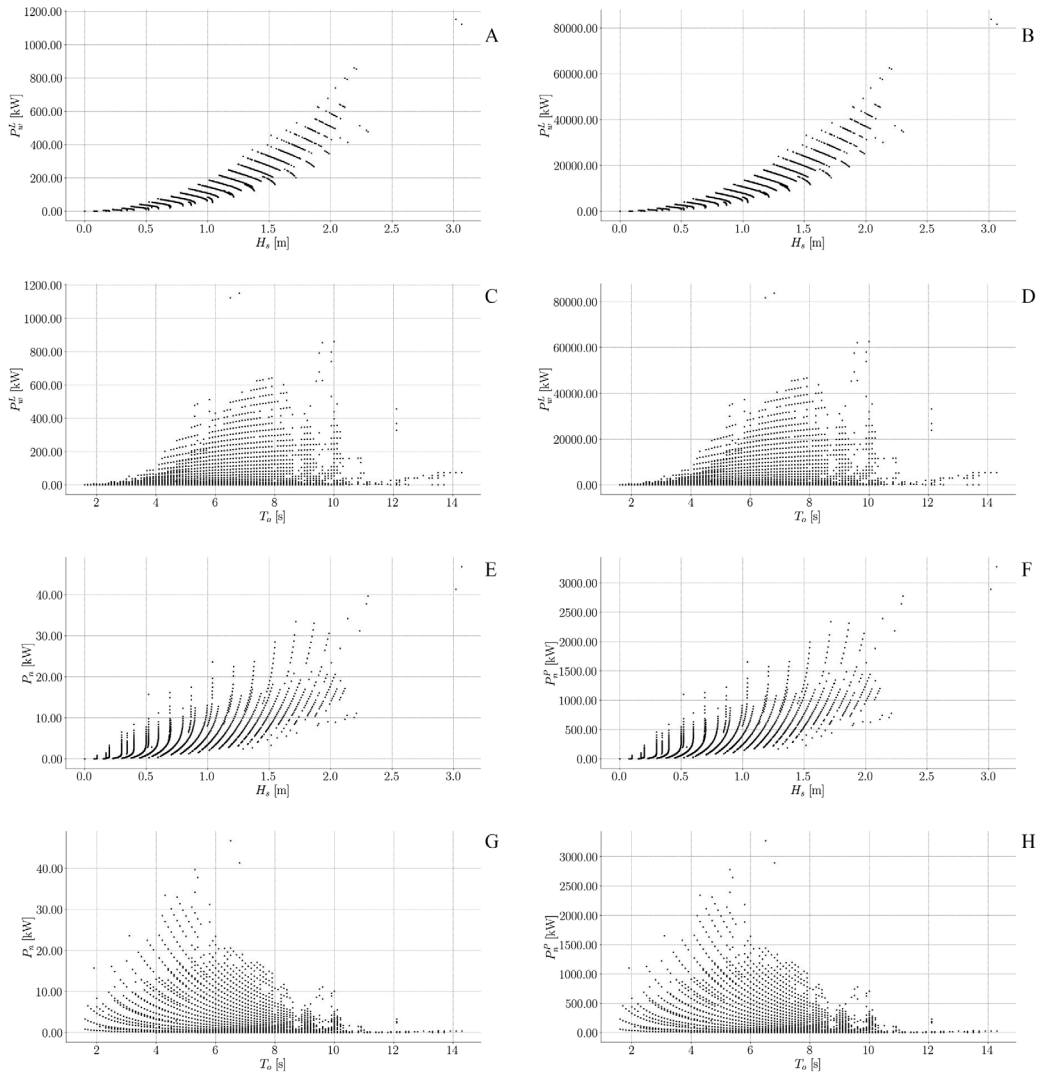

Fig. 19. OWC system. A: Power incident on a 16 m long OWC module as function of wave height. B: Power incident on a 1050 m OWC projected modules as function of wave height. C: Power incident on a 16 m OWC projected module as function of wave period. D: Power incident on a 1050 m OWC projected modules as function of wave period. E: Pneumatic power on a 16 m OWC projected module as function of wave height. F: Pneumatic power on a 1050 m OWC projected modules as function of wave height. G: Pneumatic power on a 16 m OWC projected module as function of wave period. H: Pneumatic power on a 1050 m OWC projected modules as function of wave period.

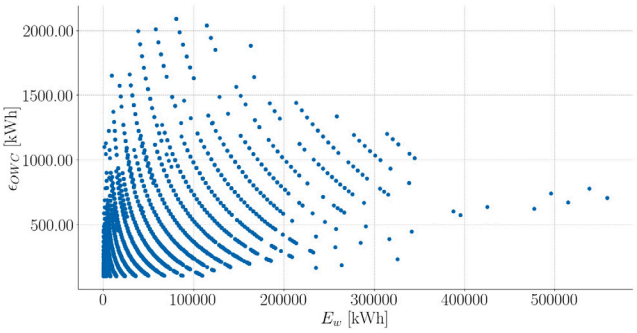

Fig. 20. Relation between incident wave energy and electrical energy obtained by the OWC system.

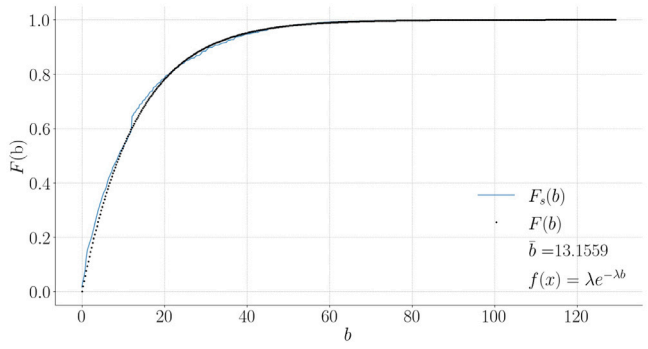

Fig. 21. Economic value of energy by sea state. Probability distribution function $F(b)$. Cumulative frequency function $F_s(b)$. Average benefit by sea state $\bar{b}$.

it into Eq. (31), it gives Eq. (33). Rearranging terms and using Eq. (29) we obtain both the extensive Eq. (34) and the intensive Eq. (35) variable function. Given an extensive variable Z, a chemical reaction responds to Eq. (36). Differentiating Eq. (34) and using Eqs. (25) and (29), rearranging terms gives Eq. (37). Eq. (36) can be written as Eq. (38) and therefore, the relationship sought corresponds to Eq. (39).

$$\left(\frac{\partial Z}{\partial T}\right)_{P,N} = -S \quad \left(\frac{\partial Z}{\partial P}\right)_{T,N} = V \tag{32}$$

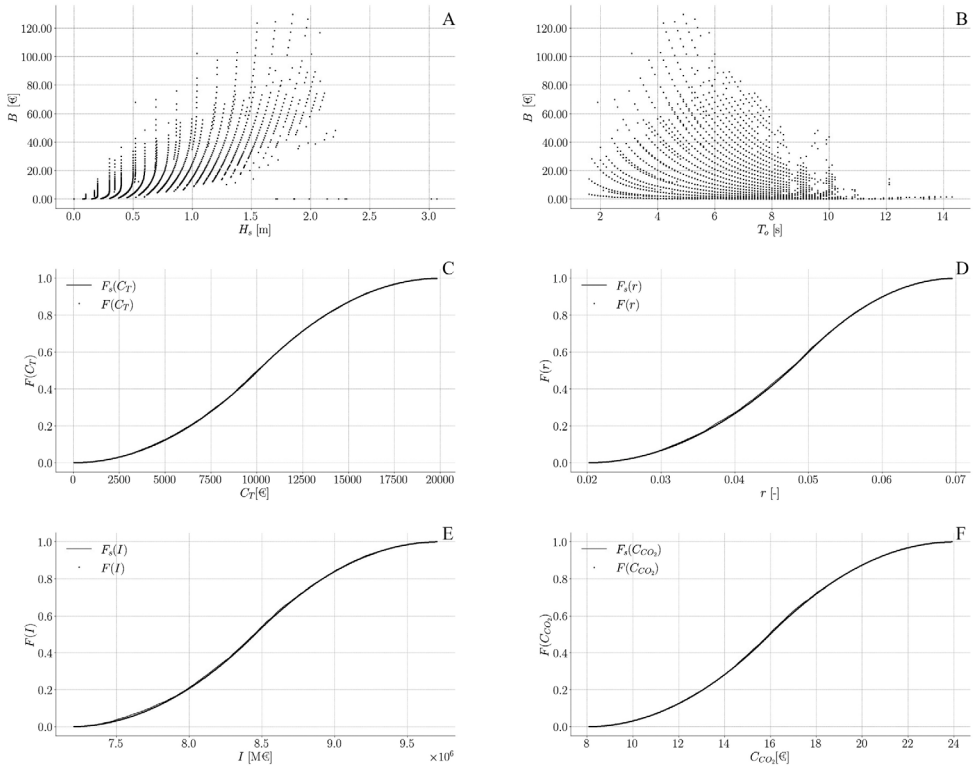

Fig. 22. Distribution functions of investment analysis. A: Dispersion of the benefits as function of height wave. B: Dispersion of the benefits as function of period wave. C: Distribution function of cost. D: Distribution function of rate of return. E: Distribution function of investment. F: Distribution function of value of CO_2 emissions.

$$Z(S,V,N_i) = -\left(\frac{\partial Z}{\partial T}\right)_{P,N_i}\left(\frac{\partial Z}{\partial S}\right)_{V,N_i} + \left(\frac{\partial Z}{\partial P}\right)_{T,N_i}\left(\frac{\partial Z}{\partial V}\right)_{S,N_i} + N_i\left(\frac{\partial Z}{\partial N_i}\right)_{S,V,N'} \tag{33}$$

$$Z(S,V,N_i) + TS - PV = Z(T,P,N_i) = \sum_{k=1}^{r} N_i z_i \tag{34}$$

$$z(s,v,x) = \sum_{k=1}^{r} x_i z_i \tag{35}$$

$$\Delta Z = Z_f - Z_i = \sum_{i=1}^{r} N_i(B) z_i(B) - \sum_{i=1}^{r} N_i(A) z_i(A) \tag{36}$$

$$dZ = \left(\frac{\partial Z}{\partial T}\right)_{P,N} dT + \left(\frac{\partial Z}{\partial P}\right)_{T,N} dP + \sum_{i=1}^{r} \nu_i z_i d\zeta \tag{37}$$

$$\Delta Z = \int_0^{\zeta} \frac{dZ}{d\zeta} d\zeta \tag{38}$$

$$\Delta Z = \int_0^{\zeta(1kg_{H_2O})} \frac{dZ}{d\zeta} d\zeta \tag{39}$$

Appendix B. Results

B.1. Equation of state

The equations of state are presented in Wagner and Pruß (2002) for water, in Leachman et al. (2009) for hydrogen and in Schmidt and Wagner (1985) for oxygen, and the reduced variables are replaced by their numerical values ($\tau = T_c/T$; $\delta = \rho/\rho_c$). The critical values of each element are expressed in Table 13. All equations are therefore a function of the density and the temperature of the system. To solve the thermodynamic cell, a range of values of temperature (T_1, T_2) and of density (ρ_1, ρ_2) are taken Table 13. The thermodynamic cells Ω_k are obtained by Eq. (40). The molar thermodynamic potential cells g (Gibbs) are shown in Fig. 17, for each studied element. Once the thermodynamic cells are calculated see Fig. 17, the equilibrium thermodynamic state defined by density and temperature is shown Table 14 with the extensive values that 1 kg of water H_2O has and its components (0.111 kg of H_2 and 0.889 kg of O_2).

Table 14
Equilibrium thermodynamic states.

Variable		H_2O	H_2	O_2	Units
Number of Moles	N	55.0	55.0	27.5	mole
Molar mass	M	18.01528	2.01588	31.9988	g mol^{-1}
Mass	m	1.0	0.11111	0.8889	kg
Pressure	p	3961482.471	100469.641	100424.366	N m^2
Entropy	S	0.294	6.259	5.678	kJ K^{-1}
Volume	V	0.001	1.346	0.673	m^3
Internal energy	U	83.0	295.829	168.7	kJ
Enthalpy	H	87.008	430.82	236.268	kJ
Gibbs potential	G	1.007	−1403.213	-1427.269	kJ
Helmholtz Potential	F	−2.954	-1538.203	−1494.836	kJ
Chemical potential	μ	0.0183	−25.513	-51.901	kJ
Isochoric molar heat	cv	4.144	1.135	0.584	kJ K^{-1}
Isobaric molar heat	cp	4.172	1.595	0.816	kJ K^{-1}
Formation Energy	pV	3.961	134.99	67.568	kJ
Caloric energy	TS	86.001	1834.033	1663.537	kJ

$$\Omega_k(\rho_i;T_j) = \{p_k(\rho_i,T_j); u(\rho_i,T_j); g(\rho_i,T_j); h(\rho_i,T_j); f(\rho_i,T_j); s(\rho_i,T_j); cp(\rho_i,T_j); cv(\rho_i,T_j)\} \tag{40}$$

Table 15
Advance in reaction ζ.

i	ν	$\zeta = 0$	$\zeta = 0.5$	$\zeta = 1$
N_{H_2O}	-2	2	1	0
N_{H_2}	2	0	1	2
N_{O_2}	1	0	0	1

Table 16
Required energy.

H_2O	Electric energy	H_2	O_2
1 kg of H_2O +	$\Delta G = 2831.48$ kJ = 0.7865 kWh	0.1111 kg de H_2	0.8889 kg de O_2

Table 17
OWC configuration parameters.

Description	Variable	Value	Units
Submerged distance	d	10	m
OWC chamber surface	S_{owc}	96	m^2
Submerged water volume	V_o	1430	m^3
Turbine parameter (Martins-Rivas and Mei, 2009)	k	0.55	[-]
Turbine diameter	D	1	m
Number of laps	N_l	$1100\frac{2\pi}{60}$	rad s^{-1}
Air density	ρ_a	1.25	kg m^{-3}
Speed of sound in air	C_s	343.2	m s^{-1}
Unit capture length	L_n	16	m
Number of OWC per unit	n_u	10	u
Turbine power	P_{tw}	30	kW
Module capture length	L_{ct}	150	m
Number of modules	n_c	7	u
Total implantation length	L_{Tc}	1050	m

B.2. Change of state

Eq. (25) is described for each studied element. Eqs. (41) for water, (42) for hydrogen and (43) for oxygen are integrated obtaining the extensive variables G (potential gibbs) Eq. (44) which is equal to electrochemical potential or energy required to disassociate 1 kg of water (see Table 15). Table 16 shows the extensible values for 1 kg of water.

$$N_{H_2O}(B) = 2 - 2\zeta \tag{41}$$

$$N_{H_2}(B) = 2\zeta \tag{42}$$

$$N_{O_2}(B) = 1\zeta \tag{43}$$

$$\Delta G = \int_0^{1kgH_2O} \frac{dG}{d\zeta} d\zeta = \|2831.488\| \text{ kJ} \tag{44}$$

B.3. Implementation of the owc system.

Fig. 18A proposes a possible configuration for the implementation of the OWC modules and the areas destined for storage and the electrolysis process in the port of Motril (Spain). This work focuses on geometric limitations and does not consider dynamic or structural implications. The projected modules of the OWC system in this work can be seen in Figs. 18B and 18C. OWC configuration and modules parameters which are been adapted to the configuration and geometry of the port are shown in Table 17.

A set of 10 turbines per module with a power of 30 kW each are planned. Therefore, a power of 300 kW per module can be achieved obtaining a total installed power of 2100 kW = 2.1 MW. Power incident on OWC modules is shown in Fig. 19AB as function of wave height, and as a function of wave period in Fig. 19CD. The pneumatic power P_n that can be extracted is shown in Figs. 19EF, 19GH as a function of wave height and period respectively. Fig. 20 shows the relation between incident wave energy and electrical energy that is obtained by the OWC system ϵ_{OWC}.

Table 18
Investment analysis values.

	Unit price considered	Estimate	Source
INV_1	4.10 M€kW^{-1}	8.200 M€	Medina-Lopez et al. (2019)
INV_2	0.0012 M€kW^{-1}	0.252 M€	Guillet and Millet (2015)
INV_{Total}		8.452 M€	

B.4. Investment analysis

To calculate ∇INV two types of investments are identified: the investment for the implementation of the OWC system (INV_1) and the installation of the electrolytic conversion system (INV_2). Following Medina-Lopez et al. (2019) and Guillet and Millet (2015), the investment costs that have been taken in this study are shown in Table 18.

The electric power generated by the OWC system plus the electric power stored in the form of hydrogen are accounted for as revenue. This energy has been multiplied by its market value. The average annual price has been obtained from the National Commission of Markets and Competition, Alonso Ba (2020). As indicated by this Commission, the minimum expected price for 2019 is 43.2 €MWh^{-1}, with a maximum of 74.73 €MWh^{-1}. Fig. 22AB shows the generated profit by the plant, considering an average price of 0.058 €kWh^{-1}.

Real observations made by 'Puertos del Estado' are used for probabilistic analysis. The function that best fits the calculated profit function is an exponential Fig. 21 with $\lambda = 1/\bar{b}$ and $\bar{b} = 13.15$ €.

Variable cost value $C_T(D_j)$ Eq. (16) has been defined following a triangular distribution, Fig. 22C. The value of the return rate r is also defined as a triangular distribution function, Fig. 22D, oscillating between 0.02 and 0.07. The investment distribution function is shown in Fig. 22E.

Emissions Trading System is a market-based instrument that creates an economic incentive for environmental benefit. The European Union launched the CO_2 market on January 1, 2005. As noted in Semprún (2019), it is a variable market, with average values varying from 8 €$Tn_{CO_2}^{-1}$ in 2017 to 24 €$Tn_{CO_2}^{-1}$ in 2019. These CO_2 emissions are taken into account following a triangular distribution, with a mean expected value of 16 €$Tn_{CO_2}^{-1}$ SENDECO$_2$, Fig. 22F.

The economic net value $NV_{eco,t}$ is calculated with Eq. (13) for the financial $NPV_{eco,t}$ Eq. (14), and the $NPV_{soc,t}$ for the social with Eq. (15). Monte-Carlo techniques are used to estimate the probable number of years in which the investment will be profitable, i.e when the $NPV_{eco,t} = 0$ or $NPV_{soc,t} = 0$. Hence, 100 simulations of 100 years each are run. Random sea states are simulated, for financial Fig. 23A and social Fig. 23B analyses. Once both are calculated, the cumulative frequency and distribution function of the payback period of each index is calculated. Fig. 23C shows the financial $NPV_{eco,t}$ and Fig. 23D shows the social $NPV_{soc,t}$. It should be noted that with a probability of 50% recovers the initial investment in 64 years for financial $NPV_{eco,t}$ while the social $NPV_{soc,t}$ takes 25 years.

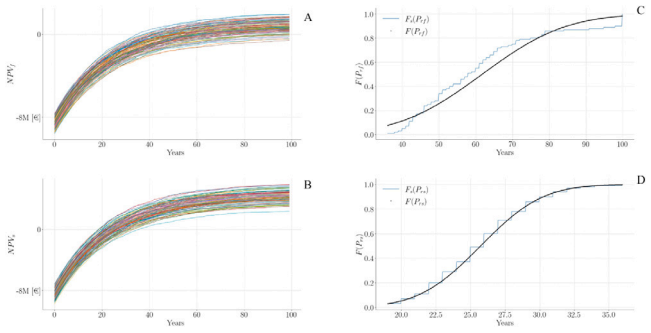

Fig. 23. Investment Analysis. A: $NPV_{soc,t}$ financial analysis. B: $NPV_{eco,t}$ social analysis. C: Distribution function for payback period in financial analysis. Probability distribution function $F(P_{rf})$. Cumulative frequency function $F_s(P_{rf})$. D: Distribution function for payback period in social analysis. Probability distribution function $F(P_{rf})$. Cumulative frequency function $F_s(P_{rf})$.

Appendix C. Nomenclature

Greek Capital Letters	
ΔZ_i:	Change of state of the ith extensive variable.
Δz_i:	Change of state of the ith intensive variable.
ΔN:	Molar increase.
ΔE_{st}:	Energy variation in the system.
$\Omega_k(\rho, T)$:	Thermodynamic state cell kth.
Lowercase Greek	
δ :	Reduced density.
ϵ_{st} :	Energy stored in the form of hydrogen.
ζ :	Progress of a reaction.
$d\zeta$:	Progress reaction differential.
η :	Efficiency.
η_{el} :	Electrolysis efficiency.
η_{OWC} :	OWC efficiency.
η_{ex} :	Exergy efficiency.
θ :	Angle of incidence.
λ_{ex} :	Renewability index.
μ :	Chemical potential, dissolved salts.
ϕ :	Dimensionless free energy equation.
ϕ^o :	Dimensionless ideal free energy equation.
ϕ^r :	Dimensionless residual free energy equation.
ρ :	Density.
ρ_a :	Air density.
ρ_c :	Critical density.
τ :	Reduced temperature.
ν_i :	Stoichiometric value ith.
Capital letters	
A :	Reagents.
B :	Products.
C :	Cost.
C_g :	Group speed.
C_s :	Speed of sound in air.
CO :	Costs.
CO_2 :	Carbon dioxide.
D :	Diameter of turbine, Damage function.
E^o :	Average spatial power.
E^o :	Ideal electrical potential.
$E_{st,t}$:	Energy stored at time t.
$E_{st,t-1}$:	Energy stored at time t-1.
E_{in} :	Energy input.
E_{in} :	Energy output.
ECL :	Customer surplus.

Capital Letters	
F :	Helmholtz free energy, renewable energy input source.
$F(b)$:	Profit distribution function.
$F(C_T)$:	Cost distribution function.
$F(I)$:	Investment distribution function.
$F(C_{CO_2})$:	CO_2 cost distribution function.
$F(r)$:	Rate of return distribution function r.
$F(P_r)$:	Payback period distribution function.
G :	Gibbs potential.
H :	Enthalpy.
H_s :	Significant wave height.
H_2 :	Molecular hydrogen; Propagated wave height.
H_2O :	Molecular water.
I :	Income.
I_ϵ :	Income from energy stored.
$\|L\|$:	Desired energy, work.
L_c :	Capture length.
L_n :	Capture length of an OWC unit.
L_{ct} :	Capture length of a module.
L_{Tc} :	Total length of capture.
M_i :	Molar mass ith molar mass.
N :	Number of moles.
N_i :	ith number of moles.
N_k :	Total number of moles.
N_l :	Number of laps.
O_2 :	Molecular oxygen.
P :	Average spatial power.
P_n :	Pneumatic power.
P_r :	Recovery period.
PM :	Market prices.
Q :	Air flow.
$\|Q_1\|$:	Necessary energy.
$\|Q_2\|$:	Unavoidable energy.
$\hat{Q}$:	Complex flow through the turbine.
$\hat{Q}^R$:	Complex flow refraction problem.
$\hat{Q}^D$:	Complex flow diffraction problem.
$Q(t)$:	Flow function as a function of time.
R :	Ideal gas constant.
S :	Entropy.
S_{owc} :	OWC chamber surface.
S_p :	Storage area.
T :	Temperature.
T_c :	Critical temperature.
T_p :	Peak period.
Capital Letters	
U :	Internal energy.
V :	Volume.
V_o :	Submerged volume.
$\dot{V}^{\zeta}_{H_2O}$:	Dissociated volume of water.
$NV_{eco,t}$:	Net value in year t.
NPV :	Net present value.
NPV_{eco} :	Financial economic net present value.
NPV_{soc} :	Social economic net present value.
Z_i :	Extensive ith variable.
Lowercase	
b :	Expected economic benefit.
cp :	Isobaric molar heat.
cv :	Isochoric molar heat.
d :	Submerged distance.
e^- :	Electron, charge.
d_{ex} :	Exergy destruction.
f :	Molar Helmholtz free energy.
$f(\delta, \tau)$:	Molar free energy as a function of reduced variables.

f^o :	Ideal free energy equation.
f^r :	Residual free energy equation.
g :	Molar Gibbs, Gravity.
h :	Molar enthalpy, bathymetric depth.
i :	Complex value.
k :	Turbine parameter.
m_i :	ith mass.
m_{st} :	Mass of stored energy.
n_c :	Number of OWC modules.
n_u :	Number of units of OWC per module.
p :	Pressure.
$p(t)$:	Pressure function as a function of time.
$\hat{p}$:	complex pressure inside turbine.
r :	Rate of return.
s :	Molar entropy.
t :	Time.
u :	Molar internal energy.
v :	Molar volume.
w :	Z component of free surface velocity; angular frequency.
x_i :	ith mole fraction.
z_i :	Intensive variable ith.
Mathematical Symbology	
∇EO :	Operators' surplus.
∇ECL :	Customer surplus.
∇INV :	Investment costs.
$\nabla(CO-PM)$:	Difference in opportunity costs.

References

Agfa, https://www.agfa.com/specialty-products/solutions/membranes/separator-membranes-for-alkaline-electrolysis/.

Alonso Ba, Beatríz, 2020. Mercado de la Energía Eléctrica en España.

Bingham, Harry B, Ducasse, Damien, Nielsen, Kim, Read, Robert, 2015. Hydrodynamic analysis of oscillating water column wave energy devices. J. Ocean Eng. Mar. Energy 1 (4), 405–419.

Blanco-Fernández, Pilar, Pérez-Arribas, Francisco, 2017. Offshore facilities to produce hydrogen. Energies 10 (6), 783.

Corrado, 2006. Environmental assessment and extended exergy analysis of a "zero CO2 emission", high-efficiency steam power plant. Energy 31 (15), 3186–3198.

Costa, R.L., Grimes, P.G., 1967. Electrolysis as a Source of Hydrogen and Oxygen. Technical report, Allis-Chalmers Mfg. Co., Milwaukee.

Cruz, Joao, 2008. Ocean wave energy. In: Current Status and Future Prespectives. Springer-Verlag Berlin Heidelberg, ISBN: 978-3-642-09431-6, http://dx.doi.org/10.1007/978-3-540-74895-3.

Da Rosa, Aldo Vieira, Ordonez, Juan Carlos, 2021. Fundamentals of Renewable Energy Processes. Academic Press.

de Oliveira Junior, Silvio, 2013. Exergy analysis and environmental impact. In: Exergy. Springer, pp. 281–303.

Engelhardt, V., 1904. The Electrolysis of Water: Processes and Applications. In: Monographs on applied electrochemistry, Chemical Publishing Company.

European Commision, 1999. Commission directive 1999/77/EC of 26 July 1999. http://ec.europa.eu/enterprise/sectors/chemicals/files/markrestr/derogation_chrysotile_asbestos_diaphragms_en.pdf.

Evans, D.V., 1982. Wave-power absorption by systems of oscillating surface pressure distributions. J. Fluid Mech. 114, 481–499.

Evans, D.V., Porter, R., 1995. Hydrodynamic characteristics of an oscillating water column device. Appl. Ocean Res. 17 (3), 155–164.

Gayé, Jesús Biel, 1997. Curso Sobre El Formalismo Y Los MÉTodos de la TermodináMica:[Volumen 2], Vol. 1,2. Reverté.

Gerken, James B., Shaner, Sarah E., Massé, Robert C., Porubsky, Nicholas J, Stahl, Shannon S, 2014. A survey of diverse earth abundant oxygen evolution electrocatalysts showing enhanced activity from Ni–Fe oxides containing a third metal. Energy Environ. Sci. 7 (7), 2376–2382.

Gilliam, R.J., Graydon, J.W., Kirk, D.W., Thorpe, S.J., 2007. A review of specific conductivities of potassium hydroxide solutions for various concentrations and temperatures. Int. J. Hydrogen Energy 32 (3), 359–364.

Grubb, W.T., 1959. Batteries with solid ion exchange electrolytes I . Secondary cells employing metal electrodes. J. Electrochem. Soc. 106, 275–278.

Guillet, Nicolas, Millet, Pierre, 2015. Fundamentals of water electrolysis. In: Hydrogen Production. John Wiley and Sons, Ltd, ISBN: 9783527676507, pp. 33–62 117–166. http://dx.doi.org/10.1002/9783527676507.ch2, URL https://onlinelibrary.wiley.com/doi/abs/10.1002/9783527676507.ch2.

Hale, Arthur James, 1919. The Manufacture of Chemicals by Electrolysis. Van Nostrand.

Holtappels, Kai, 2002. Report on the experimentally determined explosion limits, explosion pressures and rates of explosion pressure rise-Part 1: methane, hydrogen and propylene.

IEA Energy Technology Essen-tials, 2007. Hydrogen produc-tion and distribution. http://www.iea.org/techno/essentials5.pdf.

Jaynes, Edwin T., 1957. Information theory and statistical mechanics. II. Phys. Rev. 108 (2), 171.

Katrin, Bock, Stefan, Trück, 2011. Assessing uncertainty and risk in public sector investment projects. Technol. Invest. 2011.

Kreuter, W., Hofmann, H., 1998. Electrolysis: The important energy transformer in a world of sustainable energy. Int. J. Hydrogen Energy (ISSN: 0360-3199) 23 (8), 661–666. http://dx.doi.org/10.1016/S0360-3199(97)00109-2, URL https://www.sciencedirect.com/science/article/pii/S0360319997001092.

Leachman, Jacob W, Jacobsen, Richard T, Penoncello, SG, Lemmon, Eric W, 2009. Fundamental equations of state for parahydrogen, normal hydrogen, and orthohydrogen. J. Phys. Chem. Ref. Data 38 (3), 721–748.

López, I., Pereiras, B., Castro, F., Iglesias, Gregorio, 2014. Optimisation of turbine-induced damping for an OWC wave energy converter using a RANS–VOF numerical model. Appl. Energy 127, 105–114.

Lovas, Stéphanie, Mei, Chiang C., Liu, Yuming, 2010. Oscillating water column at a coastal corner for wave power extraction. Appl. Ocean Res. 32 (3), 267–283.

Luo, Yongyao, Nader, Jean-Roch, Cooper, Paul, Zhu, Song-Ping, 2014. Nonlinear 2D analysis of the efficiency of fixed oscillating water column wave energy converters. Renew. Energy 64, 255–265.

Martins-Rivas, Herve, Mei, Chiang C., 2009. Wave power extraction from an oscillating water column at the tip of a breakwater. J. Fluid Mech. 626, 395.

Medina-López, E, Bergillos, RJ, Moñino, A, Clavero, M, Ortega-Sánchez, M, 2017a. Effects of seabed morphology on oscillating water column wave energy converters. Energy 135, 659–673.

Medina-Lopez, E., Borthwick, A.G.L., Moñino, A., 2019. Analytical and numerical simulations of an oscillating water column with humidity in the air chamber. J. Cleaner Prod. 238, 117898.

Medina-López, Encarni, Moñino, Antonio, Borthwick, AGL, Clavero, María, 2017b. Thermodynamics of an OWC containing real gas. Energy 135, 709–717.

Moñino, Antonio, Medina-López, Encarnación, Bergillos, Rafael J, Clavero, María, Borthwick, Alistair, Ortega-Sánchez, Miguel, 2018. Thermodynamics of an oscillating water column containing real gas. In: Thermodynamics and Morphodynamics in Wave Energy. Springer, pp. 29–43.

Moñino, A, Medina-López, E, Clavero, M, Benslimane, S, 2017. Numerical simulation of a simple OWC problem for turbine performance. Int. J. Mar. Energy 20, 17–32.

Mundi, Index, Hydrogen produc-tion and distribution, http://www.indexmundi.com/commodities/?commodity=nickel.

Murray, Raney, 1925. Method of preparing catalytic material. US Patent 1, 563, 587.

Murray, Raney, 1927. Method of producing finely-divided nickel. US Patent 1, 628, 190.

NIST, National institute of standards and technology, https://webbook.nist.gov/chemistry/fluid/.

Puertos, Del Estado, Prediccion de oleaje, nivel del mar; Boyas y mareografos, Datos Históricos, SIMAR: 2042080 and SIMAR.

Renner, Terry, 2007. Quantities, Units and Symbols in Physical Chemistry. Royal Society of Chemistry.

Rezanejad, K., Bhattacharjee, J., Soares, C. Guedes, 2013. Stepped sea bottom effects on the efficiency of nearshore oscillating water column device. Ocean Eng. 70, 25–38.

Rezanejad, K., Bhattacharjee, J., Soares, C. Guedes, 2015. Analytical and numerical study of dual-chamber oscillating water columns on stepped bottom. Renew. Energy 75, 272–282.

ROM, 2009. 1.09 recomendaciones de diseño y ejecución de las obras de abrigo.

Rosen, 1995. Energy and exergy analyses of electrolytic hydrogen production. Int. J. Hydrogen Energy 20 (7), 547–553.

Sarmento, António J.N.A., Falcão, A.F. de O., 1985. Wave generation by an oscillating surface-pressure and its application in wave-energy extraction. J. Fluid Mech. 150, 467–485.

Schalenbach, M., Lueke, Wiebke, Stolten, D., 2016. Hydrogen diffusivity and electrolyte permeability of the zirfon PERL separator for alkaline water electrolysis. J. Electrochem. Soc. 163.

Schmidt, O., 1899. Apparat zur elektrolyse von wasser.

Schmidt, R., Wagner, W., 1985. A new form of the equation of state for pure substances and its application to oxygen. Fluid Phase Equilib. 19 (3), 175–200.

Schröder, Volkmar, Holtappels, Kai, 2005. Explosion characteristics of hydrogen-air and hydrogen-oxygen mixtures at elevated pressures. In: International Conference on Hydrogen Safety, Congress Palace, Pisa, Italy.

Sciubba, 2007. A brief commented history of exergy from the beginnings to 2004. Int. J. Thermodyn. 10 (1), 1–26.

See, Dawn M., White, Ralph E., 1997. Temperature and concentration dependence of the specific conductivity of concentrated solutions of potassium hydroxide. J. Chem. Eng. Data 42 (6), 1266–1268.

Semprún, África, 2019. El economista (empresas y finanzas). El sector energético denuncia que el mercado del CO_2 eleva el precio de la electricidad. https://www.eleconomista.es/empresas-finanzas/noticias/10070784/09/19/El-sector-denuncia-que-el-mercado-del-CO2-eleva-el-precio-de-la-electricidad-.html.

SENDECO$_2$, Precios del mercado 2019, https://www.sendeco2.com/es/precios-co2.
Teixeira, Paulo R.F., Davyt, Djavan P., Didier, Eric, Ramalhais, Rubén, 2013. Numerical simulation of an oscillating water column device using a code based on Navier–Stokes equations. Energy 61, 513–530.
The World Bank Group, Electric power consumption (kWh per capita), https://data.worldbank.org/indicator/EG.USE.ELEC.KH.PC?locations=ES.
van Troostwijk, A. Paets, Deiman, J.R., 1789. Sur une manière de décomposer l'eau en air inflammable et en air vital. Obs. Phys. 35, 369.
Vaughan, William J, Darling, Arthur H, Rodríguez, Diego José, 2000. Uncertainty in the Economic Appraisal of Water Quality Improvement Investments: the Case for Project Risk Analysis. Citeseer.
Wagner, Wolfgang, Pruß, Andreas, 2002. The IAPWS formulation 1995 for the thermodynamic properties of ordinary water substance for general and scientific use. J. Phys. Chem. Ref. Data 31 (2), 387–535.
Wendt, H., Hofmann, H., 1985. Cermet diaphragms and integrated electrode-diaphragm units for advanced alkaline water electrolysis. Int. J. Hydrogen Energy 10 (6), 375–381.
Zhang, Yali, Zou, Qing-Ping, Greaves, Deborah, 2012. Air–water two-phase flow modelling of hydrodynamic performance of an oscillating water column device. Renew. Energy 41, 159–170.